T.R.
BOLU ABANT İZZET BAYSAL UNIVERSITY
INSTITUTE OF GRADUATE STUDIES
Department of Chemistry

SOL-GEL SYNTHESIS AND CHARACTERIZATION OF Cu AND Ni DOPED Mg-Al LAYERED DOUBLE HYDROXIDES

MASTER OF SCIENCE

HAYFAA BADR ABDULLAH AL RASHID

ACADEMIC SUPERVISOR
Prof. Dr. İZZET MORKAN

BOLU, DECEMBER 2023

APPROVAL OF THE THESIS

SOL-GEL SYNTHESIS AND CHARACTERIZATION OF Cu AND Ni DOPED Mg-Al LAYERED DOUBLE HYDROXIDES submitted by Hayfaa Badr Al Rashid and defended before the Examining Committe Members listed below in partial fulfillment of the requirements for the degree of **Master of Science** in **Department of Chemistry, Institute of Graduate Studies of Bolu Abant Izzet Baysal University in 20.12.2023** by

Examining Committee Members	**Signature**
Supervisor Prof. Dr. Izzet Morkan Bolu Abant Izzet Baysal University	.....
Member Associate Prof. Dr. Erhan Budak Bolu Abant Izzet Baysal University	.....
Member Prof. Dr. Mecit Aksu Düzce University	.....

Prof. Dr. İbrahim KÜRTÜL

Director of Instıtute of Graduate Studies

ETHICAL DECLARATION

In this thesis dissertation that was properly prepared according to the Thesis Writing Rules of Bolu Abant İzzet Baysal University of the Institute of Graduates Studies, I hereby declare that;

- All data, information, and documents presented in the thesis were obtained in accordance with the academic and ethical rules,
- All data, documents, assessments, and results were presented in accordance with the scientific ethical and moral rules,
- All works that were benefitted in the thesis were appropriately cited,
- No alteration was made in the data used,
- Study presented in this thesis is original,

Otherwise, I declare that I accept the loss of all my rights in case any contradiction that may arise against me.

The similarity rate obtained by using the Turnitin program, a plagiarism detection software, is within the limits approved by the University Senate."

_____

Hayfaa Badr AL RASHID

ABSTRACT

SOL-GEL SYNTHESIS AND CHARACTERIZATION OF Cu AND Ni DOPED Mg-Al LAYERED DOUBLE HYDROXIDES
MSC THESIS
HAYFAA BADR ABDULLAH AL RASHID
BOLU ABANT IZZET BAYSAL UNIVERSITY
INSTITUTE OF GRADUATE STUDIES
DEPARTMENT OF CHEMISTRY
(SUPERVISOR: PROF. DR. İZZET MORKAN)

BOLU, DECEMBER 2023

(xiii + 51)

Layered double hydroxides are a kind of anionic clays that have unique chemical and physical properties. The objective of this work was to investigate the impact of replacing magnesium with transition metals in $Mg_{3-x}M_x/Al_1$ (M= Ni, Cu) (LDHs). A recently developed sol-gel synthesis process has been used for the production of the aforementioned materials.

The experimental findings suggested that the introduction of varying quantities of Ni and Cu into the sol-gel-derived (LDHs) did not result in the destruction of their layered structure. The sol-gel method of processing included the utilisation of metal nitrates, namely $Mg(NO_3)_2 \cdot 6H_2O$, $Al(NO_3)_3 \cdot 9H_2O$, $Ni(NO_3)_2 \cdot 6H_2O$, and $Cu(NO_3)_2 \cdot 3H_2O$, which were dissolved in deionized water as the initial substances. Additionally, citric acid monohydrate and ethylene glycol were used as complicating agents. The mixed metal oxides (MMOs) were acquired by thermal processing of precursor gels at a temperature of 650 °C, followed by their subsequent rebuilding in water to produce the LDHs. The products of synthesised were characterised by X-ray (XRD) analysis and FT-IR: Perkin Elmer's FT-IR spectrophotometer, The study revealed that the synthesis of $Mg_{3-x}M_x/Al_1$ (M= Ni, Cu) LDH from sol-gel–derived powders is extremely dependent by the concentration and kind of transition metal present.

The sol-gel synthesis method suggested for LDHs has many advantages, including its straight forwardness, capacity to produce highly homogeneous and well-crystallized end products, efficacy, cost efficiency, and adaptability to various systems.

KEYWORDS: Hydrotalcite-like compound, Layered double hydroxides, transition metals, mixed metal oxides, Chemical synthesis, Sol-gel processing.

ÖZET

Cu VE Ni KATKILI Mg-Al KATMANLI ÇİFT HİDROKSİTLERİN SOL-JEL SENTEZİ VE KARAKTERİZASYONU
YÜKSEK LİSANS TEZİ
HAYFAA BADR ABDULLAH AL RASHID
BOLU ABANT İZZET BAYSAL ÜNİVERSİTESİ
LİSANSÜSTÜ EĞİTİM ENSTİTÜSÜ
KİMYA ANABİLİM DALI
(TEZ DANIŞMANI: PROF. DR. İZZET MORKAN)

BOLU, ARALIK – 2023
(xiii + 51)

Katmanlı çift hidroksitler, benzersiz kimyasal ve fiziksel özelliklere sahip bir tür anyonik kildir. Bu çalışmanın amacı, $Mg_{3-x}M_x/Al_1$ (M= Ni, Cu) (LDHs) magnezyumun geçiş metalleriyle değiştirilmesinin etkisini incelenmiştir. Bunun için yakın zamanda geliştirilmiş bir sol-jel sentez süreci kullanıldı ve deneysel bulgular, sol-jelden türetilmiş (LDHs) değişen miktarda Ni ve Cu'nun katılmasının katmanlı yapılarının yıkımına neden olmadığı görülmüştür. Sol-jel işleme yöntemi için başlangıç maddeleri (magnezyum nitrat ($Mg(NO_3)_2 \cdot 6H_2O$), alüminyum nitrat ($Al(NO_3)_3 \cdot 9H_2O$), nikel nitrat ($Ni(NO_3)_2 \cdot 6H2O$) ve bakır nitratı ($Cu(NO_3)_2 \cdot 3H_2O$)) deiyonize su içinde çözülmüştür. Ayrıca, kompleks ajanlar olarak sitrik asit monohidrat ve etilen glikol kullanılarak; karışık metal oksit jellerinin 650 °C‘ de termal olarak işlenmiş ve ardından LDH'leri tekrar üretmek için suda yeniden işlem yapılmıştır. Sentezlenen ürünler, X-ışını (XRD) ve FT-IR ile karakterize edilmiş olup $Mg_{3-x}M_x/Al1$ (M= Ni, Cu) LDH sentezinin, geçiş metalinin konsantrasyonu ve türüne son derece bağımlı olduğunu ortaya koymuştur.

ANAHTAR KELİMELER: Hidrotalsit benzeri bileşik, Katmanlı çift hidroksitler, geçiş metalleri, karışık metal oksitler, karışık metal oksitler, Sol-jel işleme.

TABLE OF CONTENTS

LIST OF FIGURES

Page

LIST OF TABLES

Page

LIST OF PICTURES

Page

LIST OF ABBREVIATIONS AND SYMBOLS

LDHs **:** Layered double hydroxides

HTLCs **:** Hydrotalcite

XRD **:** X-ray diffraction

MMOs **:** Mixed-metal oxides

LDOs **:** Layered double oxides

DRM **:** Dry Reforming of Methane

AEC **:** Anion Exchange Capacity

SEM **:** Scanning electron microscopy

DSC **:** Differential Scanning Calorimetry

TGA **:** Thermogravimetric Analysis

MONPs **:** Metal oxide nanoparticles

FTIR **:** Fourier Transform Infrared Spectroscopy

ACKNOWLEDGEMENTS

I dedicate the fruit of my graduation and my humble efforts to those who gave me life and hope. They taught me to climb the ladder of life with wisdom and patience. Loyalty and kindness to them My father, who was tired and made an effort for me, and he left under the dirt before reaping the fruits of the planting and embracing my success. To the sea of love, tenderness and the pulse that lives in my veins, my tender mother, and to my support in this life, my dear sisters.

My dear Prof. Dr. Izzet Morkan, expressions of gratitude and appreciation are not enough and do not fulfill your right; all expressions fail to express your great role in helping others. I extend my highest words of thanks, praise, and gratitude for what you did during the years of study by lending a helping hand and continuing to give.

And I don't forget my colleague in the laboratory, Dr. Liska Fadliyani. A letter full of love and respect for your beautiful appreciation for helping me work in the laboratory. You have all the praise and sincere gratitude for what you have done for me.

1. INTRODUCTION

1.1 Background of Layered double hydroxides:

The development of novel materials has always accompanied technological progress. Nanostructures, nanomaterials and their hybrids make up a significant portion of today's technologically significant material classes. Nanotechnology or the study of producing and modifying particles with sizes between 1 and 100 nm using a variety of synthetic processes is a relatively new field of study. Nanoparticles have unexpectedly found widespread use in several fields in recent years. These fields include inorganic and organic chemistry, molecular biology, physics, material science and medicine (1,2).

Layered double hydroxides (LDHs) have garnered significant interest from academia as well as industries through recent years. This is due to their simple and environmentally friendly synthesis, non of toxicity, lower of cost, adjustability of structure and composition, high thermal also chemical stabilityand, broad-spectrum applications and high of biocompatibility. Layered double hydroxides, Inorganic of nanomaterials with two dimensions may be serve as a storage matrix for regulating the release of various anionic species, which are also referred to as anionic clays or hydrotalcite-like compounds (3,4). These LDHs were once known as hydrotalcite-like compounds because of their structural resemblances to hydrotalcite (HTLCs). Hydrotalcites $Mg_6Al_2(OH)_{16}(CO_3)$ $4H_2O$ are white hydrous minerals that form as magnesium and aluminum hydroxy carbonates or magnesium and iron hydroxy carbonates; they have a crystalline of rhombohedral structure, a low toughness (2.00) and a low density (2.06 g/cm^3). (pyroaurite). Natural hydroxy carbonates can be found as foliated, contorted plates(5).

LDHs have a layered structure according to the earliest studies on single-crystal X-ray diffraction of minerals. Each layer contains two cations with water and carbonate ions filling the interlayer gaps. Several academics, however, disagreed at first the reason for this was that despite the identification of the fundamental parts of the LDH structure that some investigators believed that the inherent features related to the structural materials of LDHs were still unknown

(6). Several aspects of the structure, including the variety of stoichiometric and potential compositional, the Anions position as well as water molecules in the interlayer galleries, the degree of arranging cations of metal contained within the layers, and the layers stacking arrangement, remain unclear and have been the subject of debate in the scientific literature (6).

The structure of brucite $Mg(OH)_2$ serves as a jumping-off point for understanding the structures of LDH compounds . The layered structure of LDH is alike to that of the mineral content brucite $Mg(OH)_2$. Therefore, researchers looked into the synthesis of LDHs and found that various first-series transition metals may be employed to make new materials with layered structures (7).

Figure 1.1 Hydrotalcites $Mg_6Al_2(OH)_{16}(CO_3)\ 4H_2O$.

1.2 History of LDH:

The existence of layered double hydroxides has been documented for more than 150 years. Hochstetter announced the discovery of hydrotalcite, the first naturally occurring metal with this particular structure, in 1842 (8). E. Manasse, in 1915 at the University of Florence (Italy), was the first to identify those carbonate ions needed for this sort of structure claiming Carbonate ions were necessary for the formation of this particular structure. He also published the quick accurate formula for hydrotalcite [$Mg_6Al_2(OH)_{16}CO_3.4H_2O$] and similar minerals with same crystal structure.

Based on their X-ray results, Aminoff and Broome identified two distinct polytypes of hydrotalcite, one with symmetry of rhombohedral and the other with hexagonal symmetry which they named manasseite in tribute to Manasse. Later in 1942, Feithnecht created LDH synthesized layered double hydroxide and dubbed the chemical "double sheeted structure" (3) in which it was supposed that a layer of one cation's hydroxide is alternated with a layer of the second cation hydroxide.

Manasse correctly determined the stoichiometry of hydrotalcite in 1915 as $[Mg_6Al_2(OH)_{16}]CO_3.4H_2O$) and in 1960s, when Allmann 1968 (9) and Taylor 1969 (10,11) conducted pioneering single crystal X-ray diffraction (XRD) studies on samples of mineral, that the main structural features of LDHs were understood. Specifically, they demonstrated that two cations occupy a layer, whereas anions carrying water molecules occupy the interlayer space.

In 1924, it was reported that the Ni-Al-LDH-based system exhibited excellent catalytic activity when the process of hydrogenation, which marked the beginning of the widespread use of these materials as catalysts (12). A patent was initially issued in 1970 (11) asserting that substances similar to hydrotalcite are excellent precursors for hydrogenation catalysts. Reichle (1986) was the first to published review article on the topic of LDH synthesis (13).

In 1988, a brief review article covering their synthesis, characterisation and prospective applications was published by (14). Nevertheless, an essential and, classical extended review paper discussing the synthesis, physicochemical characterization, and applications of both as-prepared and calcined LDH materials was published several years subsequent (3). Currently, there are numerous ongoing debates regarding potential compositions, stoichiometry, the arrangement of metal cations inside the layers, the stacking configuration of the layers, the organisation of anions, as well as the positioning of water molecules inside the interlayer galleries (6).

1.3 Structural aspects and synthesis of LDH:

Each Mg^{2+} ion an octahedron in brucite is encircled by six OH ions in an octahedral structure and the various octahedra share edges to create a two-dimensional layered endless. When trivalent cations are used in place of divalent ones in brucite, the LDHs result. This gives the layers a positive charge that is neutralised by the intercalation of anions between them. The double hydroxides have a basic nature and an excellent intercalation capacity as well as to maintain the charge balance Anions, whether organic or inorganic, are inserted between the layers and water of crystallisation is often present in the interlayer galleries (15,16). Improved catalytic activities, Fluorescence and extraction capabilities for chosen or particular analytes are just a few examples of how these intercalations might mend the characteristics of these materials (17).

Sheet-like topography characterises the vast majority of LDHs. Because of the electrostatic interactions between them, these sheets may be stacked or aggregated with ease (18). This trait reduces the active site exposure and the particular surface area both of which are detrimental to the qualities for which LDHs are recognised (19). Since they are ion exchangable, they have many of the same physical and chemical characteristics as clay (7). Anion and cation types in the interlayer space can be changed as well as the ratio between divalent and trivalent cations (20). The attractiveness of LDHs lies in the fact that it is possible to generate structures of these compounds with attributes that may be modulated (21). Despite the fact that the general formula only requires the presence of di- and trivalent cations, identical materials were produced that contained monovalent ions of lithium (22–27). It was also demonstrated that tetravalent ions may be incorporated into LDH structures. The interlayer space of a material may include water molecules, anions, and other neutral and charged moieties (28).

Further, hydrogen bonds form a complicated network that binds these different species together, where hydrogen bonding and electrostatic attraction forces work together to link the layers to the interlayer space. LDHs have a layered structure; therefore, the anions must neutralize the positive charge surplus on both octahedral layers, which are electrically balanced by two adjacent interlayers. Strongly polarised hydroxyl groups attached to trivalent cations engage with the interlayer anions to actualize the contacts between the layers and the interlayer galleries (8).

The layered structure of an LDH breaks down throughout the calcination process because of the loss of water molecules that are physisorbed between the layers and lastly, water resulting from the layering process of dehydroxylation of the layers and anions that compensate for charges chemical composition controls the temperature at which these processes occur. However, mixed-metal oxide is often formed at temperatures above 400 °C (29,30).

When LDHs are processed, they transition into (MMOs) that have basic characteristics with a high specific area of surface. Memory effects are a characteristic of MMOs that allow them to recover their originally layered structure (31,32). Through variations in calcination temperature as well as metal constituents, the chemical characteristics of MMO derived from LDH may be controlled (33,34). As a result, MMOs synthesised using this approach find widespread use in a variety of contexts, for example, as electrochemical capacitors, antimicrobial activity, adsorbent and catalysts (35–42). The structure is porous through the process of gasification, which results in a very large specified area of surface, which is one of the distinguishing characteristics of MMO generated from LDH.

As a result, it has been reported that LDH-originated MMO has a high anionic removal capability (43,44). Although the mechanism by which LDH transforms into MMO remains unclear, Nevertheless, it is widely acknowledged that interstratified M(II)O domains developed, which are interconnected by M(III)O tetrahedra. Based on the literature study, we may propose two potential causes of porosity in MMO obtained from LDH. First, calcined LDH is used to maintain the structure of the original LDH, in which many M(II)O domains are

spaced apart at an optimal spacing. Second the presence of intraparticle space between M(II)O domains is the primary cause of porousness. Second, the calcination process causes the formation of agglomerates in MMO particles, whereby the interparticle space creates pores (45). In certain cases, calcination may be employed as a transitional treatment to modify clay as introducing anions into the interlayer by intercalation. This new level of functionality greatly enhances the usefulness of the memory effect. In aqueous solutions or a humid air environment, the oxide undergoes a retrotopotactic transformation, called the memory effect, that returns it to its original hydrotalcite structure (24). Following calcination, LDHs are converted to layered double oxides (LDOs), the major component of which might be spines or mixed metal oxides.

LDO has the "memory effect," which indicates that with rehydration and the concomitant inclusion of anions into the interlayer from an aqueous solution, this calcined product may restore LDH's original layered structure. LDOs have a large surface area and the ability to catalyse a wide range of chemical reactions involving metal cations (46). Moreover, during reconstruction, mixed oxides could absorb cations aqueous (47). This makes it feasible to create catalysts that combine hydrotalcite with particular catalytic characteristics (48), Such that LDH-derived mixed oxides rehydrate with a wide variety of metals and anions through a "memory effect," leading to a wide Scattering of active response metal particles (49).

As a result of the calcination process, LDH solids yield amorphous mixed oxides with characteristics including homogenous dispersals of metallic phase, a high surface area and tiny crystallite (50) and fundamental properties, traits that are composition-dependent (51). Following the reduction process, these materials produce stable metallic particles that are dispersed high and resistant to sintering (52,53). Due to these characteristics, these oxides are used as catalysts in many catalytic interactions (54,55), including the Dry Reforming of Methane (DRM) (56–59).

LDH compounds have typical three structural properties (Figure 1.2) ; Metal ions on the layers, Nanosheet structures and Anions in the interlayers. Depending on these properties, certain behavioural adjustments may be done (60).

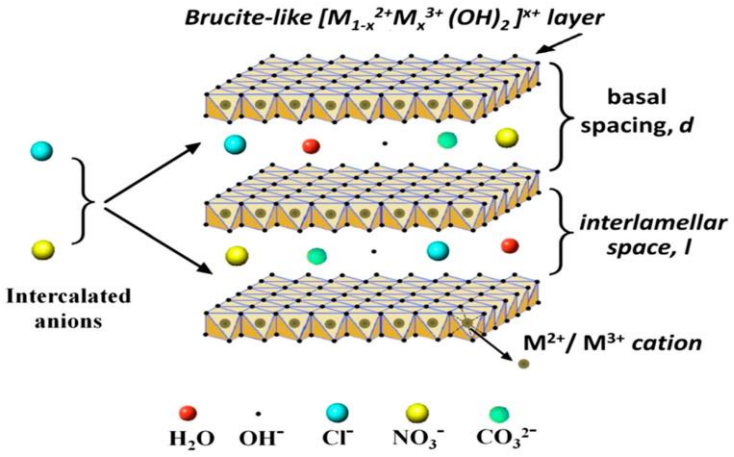

Figure1.2 General Chemical structure of double hydroxide (LDH) (61).

1.3.1 Metal ions on the layers:

The basic formula utilised in LDH materials is the metal ions on layers. $[M^{+2}{}_{1-x}M^{+3}{}_x(OH)_2]^{x+}$ $[A^{n-}]_{x/n}$ $.mH_2O$, where M hydration number is bivalent or trivalent cations having comparable radii and A are interlayer anions such as halide, nitrate, sulphate, or carbonate, countering positive charge, n is the anion charge, and the value of x, typically ranging from 0.20 to 0.36, represents the proportion of trivalent metal that substitutes the divalent metal in the layers. (62,63). Also Hydroxide layer charge density, denoted by x, is calculated using the following formula (64,65):

$$X = \frac{\text{Total charge of the trivalent cations (viz.[M3+])}}{\text{Total positive charge of the LDH nanosheet (viz.[M3+] + [M2+])}}$$

All HTs are thought to originate from hydrotalcite, a mineral that forms in nature with a composition of $Mg_6Al_2CO_3(OH)_{16}.4H_2O$ and a crystal structure very similar to that of brucite [Mg $(OH)_2$].

In these compounds, the layered crystal structure is very variable, depending on the nature of the cation, anion types and the M^{+2}/M^{+3} molar ratios (66). The optimal ratio of M^{2+}/M^{3+} to produce LDH molecules is between 2:1 and 4:1, with x in the range $[0.2 \leq x \leq 0.33]$. The creation of $M(OH)_3$ occurs when the number of neighboring M^{3+} containing octahedra increases to more than about $x > 0.33$, while the formation of $M(OH)_2$ occurs when the number of neighboring M^{2+} containing octahedra increases to more than about $x < 0.2$ in the brucite-like sheets.

Nevertheless, depending on the compostion of the LDH, these x-value bounds must be thought of as the maximum interval, which may be narrower.

Both the M^{2+} and M^{3+} cations as well as the interlayer anion are amenable to substitution or partial replacement resulting in a wide range of alterations to the material's chemical and physical characteristics. Mg^{2+}, Zn^{2+}, CO^{2+}, Ni^{2+}, Cu^{2+}, or Mn^{2+}, and Al^{3+}, Cr^{3+}, Co^{3+}, Fe^{3+}, V^{3+}, or Y^{3+} are the most prevalent M^{2+} and M^{3+} cations in the LDH structure. The majority of the time, smaller anions with a higher charge density are preferred (67–69). Monovalent anions may be exchanged more easily in the sequence of $OH^- > F^- > Cl^- > Br^- > NO_3^-$. Divalent anions, such as $SO_4^{2-} > CO_3^{2-}$, are more selective than monovalent anions. Due to their ease of removal from the interlayer, LDHs carrying NO_3 anions are the best candidates as precursors for anion exchange (70).

Compared to clays and other layered materials, LDHs are often more desirable. This is because different metal-ion combinations and compositions may be formed in LDHs during their synthesis. Furthermore, the high charge density of LDHs is a significant factor in why people prefer them over clay. The density of the LDHs' charges is set by the relative abundance of the divalent as well as trivalent metal cations. An increase in charge density is seen at low divalent/trivalent ratios (63).

1.3.2 LDH nanosheets:

There has been a lot of interest in LDH nanosheets recently. LDH nanosheets are very useful for both basic research and the construction of functional nanocomposites because of their 2D anisotropy which allows for a thickness of roughly 1 nm and a lateral dimension of tens to 1000 of nm (71). Delamination of LDH nanoparticles and direct synthesis of LDH monolayers are two methods that may be used to create LDH single sheets. The one-step synthesis process utilizes a reverse microemulsion strategy (72,73) and delamination of LDH nanoparticles may be accomplished using a broad range of solvents such as formamide, butanol, acrylates, etc (74–76).

A variety of nanoarchitectures, nanoconjugates, and nanofilms, may be created by assembling the charged nanosheets, and these materials have a wide

range of potential uses in energy storage, energy conversion, and biomedicine (77,78).

1.3.3 Interlayer Anions:

Anions in interlayer space have a wider range of options. If the metal ions are not removed from the hydroxide layer and there is a suitable charge density in a particular region, there are no limitations on the sort of anions that may be used in LDHs:

1- some biochemical anions.

2- complex anions.

3- heteropolyoxometalates and iso polyoxometalates.

4- oxygenates, sulfates, diverse organic carboxylates, and sulfonates.

5-common inorganic anions.

6- polymeric anions (63).

Within the brucite-like layers, it can be found a wide variety of anions, each with its unique structure, size, and charge. Interlayer spacing, which in turn is determined by layer size and orientation, controls layer spacing. Planar CO_3 and NO_3 anions align with the brucite-like layer for small x values, but at high x values, they tilt or alternate between an upper and lower position. This is because anions interact with their surroundings, creating a congested exhibition space (79–81).

1.3.3.1 The nature of the anion:

The positive charge on the brucite-like sheet may be neutralized by nearly any kind of anion; the only possible difficulty lies in purifying or crystallizing the material. During the process of making an anion containing LDHs, for instance, preventing contamination from carbon amounts in the aqueous solution is exceedingly challenging is exceedingly challenging to when making LDHs with anions other than carbonate. The following cations may be found in LDHs:

1- Organic acids: succinic, chlorocinnamic acid, 1,1, 2- dodecane dicarboxylic acid, oxalic, acyl, and arylsulphonates, malonic, adipic, sebacic (82–84).

2- Inorganic anions: $[Fe\ (CN)_6]^{4-}$, $(SO_4)^{2-}$, $(CO_3)^{2-}$, $(OH)^-$, $(l0_3)^-$, $(C1O_3)^-$, $(NO_3)^-$, $(C104)^-$, F^-, Cl^-, Br^-, I^-.

3- Heteropolyacids: $(PMo12040)^{3-}$, $(P\ W12040)^{3-}$ and others.

The interlayer thickness is dictated by the volume, direction, number and force of the linkages between the anions and the hydroxyl groups found in the brucite-like layers. In the interlayers, the oxygen atoms related to carbonate and water are arranged in clusters at certain locations near the symmetry axes that pass via the hydroxyl ions of the surrounding brucite layers (85,86). The carbonate group consists of the carbon atom in the center and three oxygen atoms from three groups of nearby sites. Hydroxide, nitrate, chloride, and carbonate LDHs all have a very similar interlayer arrangement (87,88).

Carbonate has been linked to strong hydrogen bonding in carbonate containing LDHs, which may explain why the interlayer thickness measured with carbonate is approaching that seen with monovalent ions (halogens) (89). Nevertheless, HTlcs containing interlayer nitrate ions have been shown to act oppositely (70) demonstrate a high repulsion with increasing NO_3^- concentration. This is because more monovalent ions are required to compensate for the positive charge, and they take up more space than other monovalent ions do.

1.4 Properties of LDH:

Nanoparticles have novel and enhanced properties, such as the distribution of particle size as well as its shape, that are not seen in bulk materials with bigger particles (90). Considering recent advances in material chemistry and nanotechnology, researchers have been able to create a wide range of nanocomposites by fusing distinct nanomaterials or altering nanomaterials with functional molecules. The nanocomposites that were made have desirable and unique properties that make them good candidates for use in cleaning up the environment, improving health care and storing and converting power (61,91–96).

The ability to mass-produce sophisticated low-dimensional compounds blocks like nanoparticles, nanorods and nanosheets, which can then be built and put together into working three-dimensional networks is key to making cutting-edge devices (20). Many attractive chemical and physical features of LDHs may be attributed to their distinctive molecular nanostructures, including flexibility, tunability, thermal stability, and interlayer spaces.

Accordingly, they are widely used in energy storage, sample preparation, catalysis and other fields (97). They can be used as an acid base (98), barrier materials (99), high-performance catalytic materials (100), memory effect (101), biodegradability (64), biomaterials (102), because of their characteristics in terms of interlayer anion exchange (103), adsorption materials (104) and separation materials (105), pH dependent solubility (106), less-toxicity (107–109).
Different LDHs show a wide range of features because of their unique builds and production methods.

1.4.1 Anion Exchange Capacity:

In the case of LDH, the Anion Exchange Capacity (AEC) is determined by the metallic cation ratio, the capacity of the involved anion to maintain lamellar structure, and the molecular masses of the cations and anions. AEC values may vary between 200 and 450 cmolc kg-1(110). Values below 200 cmol kg-1 are not feasible if the M^{2+} to M^{3+} ratio is too low to sustain LDH structure.

1.4.2 Colloidal properties:

In systems characterized by colloidal properties and/or delamination low charge density and the tiny particle size of certain LDH are crucial (Stacking structure loss). Anion interlayer diffusion issues are often seen when the host anion is big in size. An improved integration of the lamellae between the host and anion is therefore made possible by colloidal and delaminated systems, which are generated from LDH to solve these issues. By mixing LDH with organic molecules many studies have shown the emergence of systems having colloidal characteristics (110,111). Transparent and continuous films have been made from LDH colloidal suspensions (112).
Hydrotalcite and anionic surfactants, including toluene, heptane, propanol and benzene were mixed to create LDH with colloidal features and hydrophobic properties.

1.4.3 Morphological properties:

LDH may be described in terms of its physical features including shape, porosity, particle size and surface area which of course can determine its uses. Traditional LDH preparation techniques allow very little manipulation of these

features. The morphology of these substances may be evaluated using a scanning electron microscope (SEM). The specific surface area of LDH relies on both the techniques and circumstances of synthesis in addition to being connected to the component cations and anions. The LDH surface area might be anything from 50 to 200 m^2 g^{-1}, depending on the substance. The specific surface area of the oxides and/or mixed oxyhydroxides that may arise by calcining LDH under the right circumstances is much higher than that of the precursor LDH.

LDH porosity often spans the microporous to the mesoporous range (113), however, this is not always the case, proving that MgAl-LDH and colloidal polystyrene crystals may be used to create macroporous materials (PS). Using PS beads as a mold and the open 2-D structure of LDH as the "wall," 3D macroporous materials may be fabricated. (Filling the gaps between the PS beads). Calcination results in a three-dimensional macroporous structure as shown by X-ray diffraction (XRD) and scanning electron microscopy (SEM) imaging. Variations in composition and crystallinity may cause significant size variations in LDH particles. It's also worth noting that different particle size measurement methods may provide different results for the same materials. Using the peak width at half-height (or FWHM, for Full Width at Half Maximum) measured from diffractograms crystallite sizes may be calculated using the Scherrer equation (114). Particle size may also be measured using transmission electron microscopy (TEM), scanning electron microscopy (SEM), and laser scattering.

1.4.4 Thermal stability:

LDH also has the advantage virtue of being very stable at high temperatures. Differential Scanning Calorimetry (DSC) and Thermogravimetric Analysis (TGA) are used for the description of the thermal characteristics of these materials. Temperatures required for thermal breakdown vary depending on several variables including nature, the M^{2+}/M^{3+} cation molar ratio, LDH crystallinity and the interlayer anion type (Organic or inorganic).

Table 1.1 Advantages and limitations of LDH (115).

Advantages	Limitations
1- Although LDH may be found in nature, a synthetic analogue can be created. 2- Anions of varying sizes may be intercalated between the interlamellar gaps of LDH because of its high anion-exchange capacity. 3- Under certain circumstances, it can release the intercalated material slowly over time. 4- It has a wide range of uses, including fabric modifiers, various add-ons, fillers, ceramics, and so on. 5- Adsorption and intercalation may be utilized to remove hazardous chemicals from water, making this material useful for environmental remediation.	1- To properly synthesize LDH, the ratio of divalent to trivalent cations must be between 2:1 and 4:1. LDH does not form outside of this ratio's range. 2- If the precursor was calcined between 300 and 500 degrees Celsius, reconstruction, or the so-called memory effect, will be possible. As the temperature rises over this range, LDH becomes a stable spinel structure and cannot return to its former structure. 3- Since LDH are stable in neutral and alkaline pH ranges but soluble in acidic pH, its composites are ineffective in acidic environments.

1.5 LDH synthesis :

Natural occurrences of the substance are possible however, it may also be synthesised using cost-effective and friendly to the environment chemical processes (Green chemistry). This section defines the primary methods used for producing LDH nanoparticles. The synthesis of LDH requires careful consideration of various factors, including the extent of cation substitution of M^{2+} by M^{3+}, the nature of cation and interlayer anion, the synthesis pH, and, in certain instances, atmospheric control, the pH while adding (for constant-pH methods), The concentration of the solutions, the amount of stirring, the rate at which one solution is added on top of another, the final pH of the suspension (for variable-pH methods) and the temperature of the final solution which is typically carried out at room temperature must all be controlled for more crystalline materials. There exist multiple techniques for the synthesis of LDH that can be classified into two distinct categories.

The direct synthesis methods encompass several techniques, namely salt-base or coprecipitation, sol-gel, salt-oxide, hydrothermal synthesis, electrochemical preparation, and induced hydrolysis (13,116–119). Indirect synthesis methods: The involves restoring forming the calcined material as well as exchanging anions utilising a double-phase system, resulting in the creation of salts inside surfactants (120,121). Some of the most common approaches to synthesis will be discussed here.

1.6 Preparation of LDH powders:

Co-precipitation, anion exchange, calcination reconstruction, hydrothermal synthesis, and sol-gel, are all viable routes to producing LDH powders. This section demonstrates the unique features and workings of the approaches.

1.6.1 Co-precipitation:

Low saturation coprecipitation is the most common technique of preparation. The solutions of metal salts are combined in certain proportions (122). The pH of the combined salt solution is then adjusted by adding an alkali solution (often NaOH) drop by drop until the desired value is obtained. The product is aged by being stirred regularly before being filtered, cleaned, and dried. This method is simple to implement. However, this approach often does not provide well-structured LDHs.

1.6.2 Ion-exchange:

The ion exchange strategy relies on a preexisting LDH that has a guest anion that can be easily swapped out through the interlayer (123). When the native anion is switched out for a new guest species, a novel LDH is produced. This procedure is often quite simple to carry out. The procedure may occasionally be inefficient due to incomplete processing of the transaction.

1.6.3 Hydrothermal synthesis:

Hydrothermal synthesis involves a thermal aging process after co-precipitation or ion exchange, as described in reference (124). The objective of hydrothermal aging is to enhance the crystallization of the LDH. The technique has the potential to yield LDH sheets that are well-structured. It is important to note, however, that the duration of the reaction must be carefully calibrated, as prolonged reaction times can lead to an increase in the size of the LDH sheets.

1.6.4 Calcination-reconstruction:

The recovery technique of calcination relies on the "memory effect" of LDHs, as documented in reference (125). After a calcination procedure, interlayer anions like CO_3^{2-}, NO_3^-, and other organic molecules may be eliminated. As a result, the LDH collapses into a cubic phase and is transformed into a layered double oxide (LDO). A new form of LDH is produced, however, when the LDO is dissolved in water and the layered structure is recreated with a different species intercalated.

Table 1.2 Advantages and disadvantages for methods LDH powder preparation (126).

Method	Advantage	Disadvantages
1- Co-precipitation	♦ Simple equipment. ♦ One-step synthesis. ♦ Flexibility to obtain desired LDH.	♦ Formation of insoluble Compounds. ♦ Needs further crystallization.
2- Anion-exchange	♦ Avoids the formation insoluble compounds. ♦ Mild reaction conditions.	♦ Neutral species cannot be Intercalated. ♦ Two-step synthesis. ♦ Requires an alternative technique of preparing the precursor (often LDH-$NO3^-$).
3- Hydrothermal method	♦ Easy operation ♦ Simple reactant	♦ Long reaction time. ♦ High temperature.
4- Calcination-Reconstruction	♦ LDH intercalation with any anions, such as $CO3^{2-}$ is possible with the original reactant. ♦ Utilize the impact of structure memory effect ♦ Intercalation of neutral species is possible.	♦ Time-consuming ♦ Metal oxide activity determined the process of reconstruction. ♦ Requires LDH precursor synthesised using other methods.

1.6.5 Sol-gel process:

High-quality MONPs and mixed oxide composites may be prepared using the well-known sol-gel process, which is one of many recognized synthetic procedures. Gel formation is one of the steps in this procedure, which allows for precise manipulation of the final product's texture and surface qualities and is a hybrid of many different approaches to material synthesis from solution. Controlled hydrolysis of compounds (typically alkoxides M (OR) Si, V, Zr, V, Mo, Al, Sn, W, Zn, Ge, etc.) in an organic or aqueous media is the basis of one of the most common types of sol-gel synthesis (127). The sol-gel approach allows for the efficient and low-priced synthesis of HT with a high purity level. At normal temperatures, metallic precursor salts or their organic constituents are hydrolysed in water or organic solvents. In the case of insoluble salts, however, higher temperatures are necessary. To make such materials soluble, a different solvent is sometimes utilized. The sol is created from metallic, organometallic, or alkoxide precursors, following which sol undergoes a phase change to form the final product. Wet gel is formed when the acquired sol, a solution of particles in suspension, polymerizes at low temperatures (128). The dry gel is formed after the solvent is removed by conventional heating. Adding a base or an acid to the hydrolyzing solution speeds up the peptizing process, which is necessary for getting highly distributed metals in the solution (129).

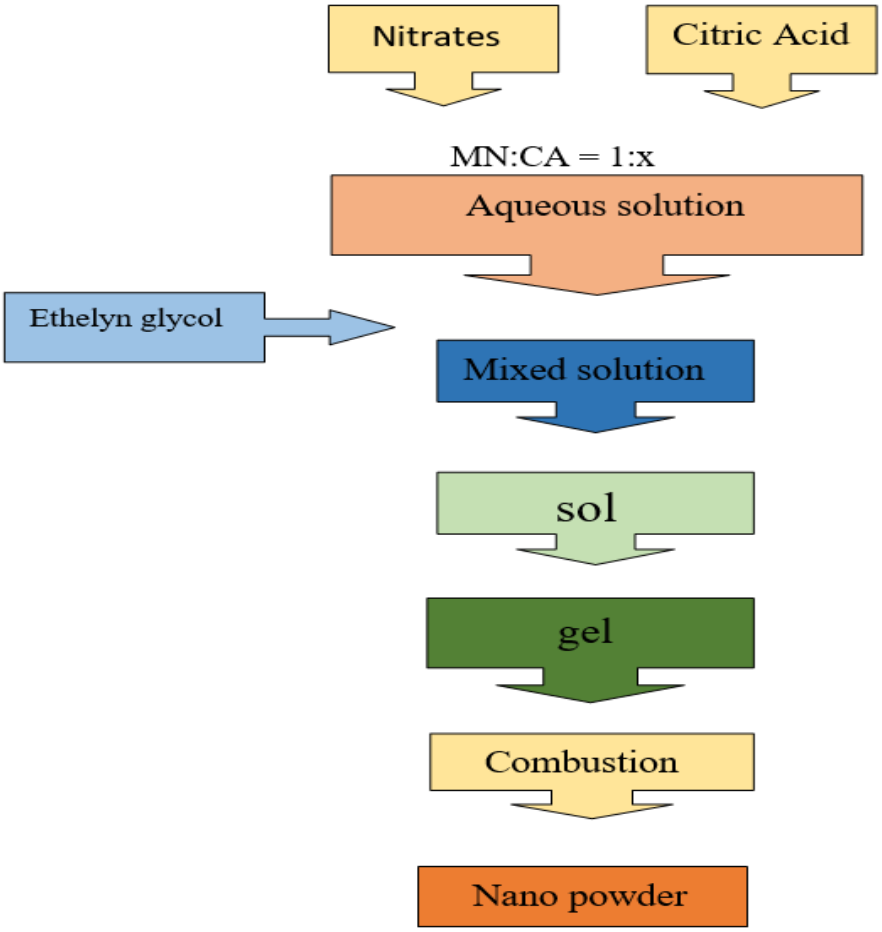

Figure 1.3 Schematic representation of the sol-gel autocombustion procedure.

-Hydrolysis, polycondensation, aging, drying, and heat degradation are the five main stages that make up the sol-gel technique (130).

1- Precursors, like metal alkoxides, undergo hydrolysis in water or alcohol. Water or organic solvents provide the oxygen needed to create metal oxide during MONP production. (e.g., alcohol). It is called an aqueous sol-gel technique when water is employed as the reaction media, and a nonaqueous sol-gel approach when an organic solvent is utilized. The hydrolysis of the precursors requires not just water and alcohol, but also an acid or a base. The following is a description of the overarching chemical reaction that occurs during hydrolysis:

M-OR + H_2O → MOH + ROH (Hydrolysis) where M=Metal, R=Alkyl group

(C_nH_{2n+1}), The quantity of water has a significant impact on how the gel forms; more water promotes the creation of a larger ratio of bridging to nonbridging oxygens, which results in a more polymerized and branched structure during condensation (131).

2- The process of condensation between adjacent molecules is essential for the removal of water and alcohol, the creation of metal oxide bonds, and the enlargement of polymeric networks into colloidal dimensions inside a liquid. Olation and oxolation are two types of condensation. Both olation and oxolation include the formation of a bridge between two metal atoms; olation involves the formation of a hydroxyl (-OH-) bridge, while oxolation involves the formation of an oxo (-O-) bridge. (Metal–oximeter bonds). The following is a description of the overarching chemical reaction that occurs during condensation:

M-OH + XO-M → M-O-M + XOH, where M=Metal, X=H or alkyl Group (C_nH_{2n+1}). The end outcome of condensation or polycondensation is an increase in solvent viscosity that creates a gel-like liquid phase with a porous structure. The alkoxide precursor and pH of the solution have a major role in determining the size and cross-linking of the colloidal particles (132–135).

3- The gel's structure and properties are a result of the process of aging, which is responsible for these changes. During the aging process, polycondensation occurs inside the confined solution, concurrently with the reprecipitation of the gel network. Because of this, eventually, the porosity of the space between the colloidal particles will decrease while the thickness of the space will rise off the gel network (136).

4- When water and organic components separate to produce a gel, the drying process becomes more difficult because the gel disrupts the original structure. Drying methods may have a significant impact on the gel network's structure in many ways. These methods include supercritical drying, freeze-drying, and thermal drying atmospheric by heating the porous gel to high temperatures, densification occurs (137). By removing the pores from the gel, xerogel is created, which has pore volume and a low surface area, and substantial shrinkage of the gel (138). Supercritical drying, on the other hand, results in the formation of aerogels with a large pore volume and surface area while the original gel network

is mostly preserved. Cryogel, the third kind of drying, is created by freezing the solvents; its gel network shrinkage is less than that of xerogel. Nanomaterials' durability and functionality are also directly influenced by the drying environment's relative humidity (RH). Nanofilms that are dried at lower RH exhibit greater stability than those dried at higher RH (139).

5- To remove any remaining materials and water molecules from the desired sample, heat treatment or calcination is lastly used. The temperature used during calcination is a crucial factor in determining the material's density and pore size.

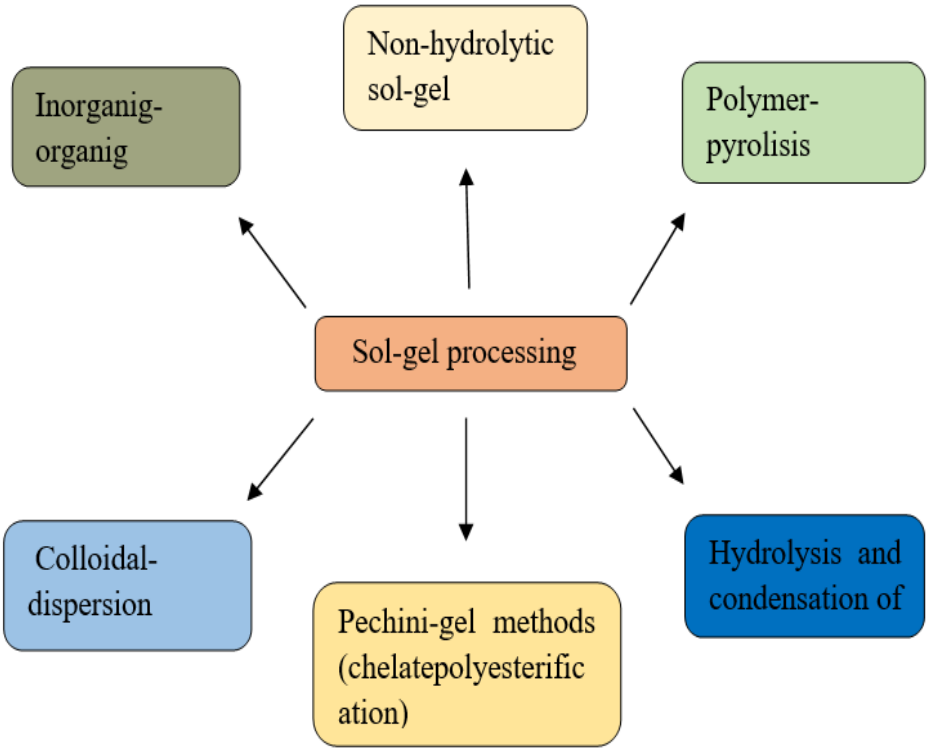

Figure 1.4 Different routes of sol-gel processing (173).

1.6.5.1 Advantages of Sol-Gel:

Increased topcoat-with-substrate bonding, when substances are in a gel condition, they are more amenable to being shaped into intricate patterns. The sol-gel transformation uses ceramic oxides as a precursor, which are dissolved in a suitable solvent to produce high-purity products. It's a procedure that just requires a low-temperature range (200-600 degrees Celsius). This technique for making high-quality coatings is easy, cheap, and efficient (140).

1.6.5.2 Disadvantages of Sol-Gel:

The sol-gel method is not capable of realizing its full commercial potential because of several constraints. Some of them have poor wear resistance, high permeability, poor bonding, and difficult porosity control. Crack-free properties have a coating thickness limit of 0.5 m. The heating process may ruin thick coatings. The temperature mismatch and surface dependency now provide a challenge for sol-gel technology. One of the primary limitations of this technique is a lack of scientific knowledge of this complicated interaction (141). One disadvantage of the sol-gel approach is the high cost of raw ingredients, drying, and sintering, as well as the lengthy procedure (142–145).

1.6.5.3 Improvement and Advancement in sol-gel Technique:

When using the sol-gel method for practical purposes, gel drying is an essential step. Kistler pioneered the study of supercritical drying(146), which resulted in the creation of aerogels with a particle capacity as high as 99.8 percent. Doping sols with chemical compounds led to the finding of miscellaneous materials. Recently developed sol-gel materials are the result of chemical synthesis in coordination chemistry (147).

One significant problem is creating materials with various surface functions, such as causing hydrophobicity. Grafting is also needed, as is chemical fixation via chemical substances that include enzymes, molecular catalysts, or other biomolecules. Organic compounds with the ability to polymerize gel can be used to create inorganic-organic composite materials with novel characteristics.

1.6.5.4 The effect of pH on sol gel technique:

The acidity or basicity of the solution (pH dependent) has a major impact on particle size and entanglement. Van der Waals interaction is important because of the tiny particle size; it grows exponentially as the particle size lowers. These factors encourage the formation of clusters.

The sample must be preserved in a powder morphology with a large surface area; hence gel stabilization is required. When the pH is low, a positively charged transition state is produced, and the alkoxide's -OR groups are more effective in stabilizing the solution than the -OH groups. Long, unbranched chains and large particles are what you should expect to see most of when working with low hydrolysed species because of their rapid condensation velocity. In contrast, the production of highly branched chains and tiny-sized particles is fevered by the quicker condensation of the high-hydrolysed species when the catalyst is basic because the transition state charge is negative and the -OH group stabilizes the solution (148,149).

1.6.5.5 Applications Sol-Gel Process-Prepared Nanomaterials:

1- Materials with altered physical characteristics, including low heat expansion rate, low UV absorbance, as well as high visual clarity, can be manufactured.

2- composite oxides are created through the synthesis of uniform materials.

3- Fabricating receptive permeable structures for organic and polymer chemical addition.

4- The potential for designing chemical compositions and achieving homogeneous compositions.

5- Extremely high productivity.

6- manufacturing complex-shapes optical components.

7- Manufacturing high purity products.

8- Precursors are highly reactive chemically because the procedure occurs in solution.

9- The product's adaptability to novel applications like filaments, aerogels, and coatings.

10- The process of synthesizing is at a low temperature.

11- The ability to use this method to synthesize as well as apply them to thin layers.

12- Controlling the materials structure precisely with the ability to modify factors during TB early stages and network development; high-quality output; Low initial investment (150,151).

1.7 Applications in practise of LDH:

Studies into the applications of LDHs are continuous and expanding. Until now, LDHs have been extensively used in several fields and span across multiple disciplines, such as, sorbents, Electrocatalysts, energy storage, drug delivery, Catalytic, memory, sensor, Photocatalyst. Nevertheless, many of these applications are constrained by the fact that host layers surfaces interiors cannot be reached.

Table 1.3 Practical Applications of LDHs.

Type of LDH	LDH synthesis method	Application of LDH	References
MgFe-Cl-C-12-LDH	Co-precipitation	Sorbents	(152)
NiLa-LDH NSAs	Electrochemical	Electrocatalysts	(153)
ZnAl LDH/CNTs	In-situ	Energy storage	(154)
Pt/C@NiRuCe-LDH	Solvothermal	Catalytic	(155)
Zn/Al-LDH@SiO_2	Sol-gel	Drug delivery	(156)
FeCoNi-LDH	Ion-exchange	Catalytic	(157)
C/NiFe-LDH	Hydrothermal	Adsorption	(158)
ZnNiCr-LDHs	Microwave hydrothermal	Adsorption	(159)
Nb-NiFe-LDH	Salt-oxide	Catalytic	(160)
ZnAl-LDHs	Reconstruction	memory, sensor	(161)
NiAl-LDH/g-C_3N_4	Urea method	Photocatalyst	(162)

2. AIM AND SCOPE OF THE STUDY

The main aim of this work is the sol-gel synthesis and characterization of double metal-substituted $Mg_{3-x-yM\times}M'_y/Al_1$ (M=Ni and M'=Cu) LDH films. For that purpose, four different compositions of LDHs structures are chosen. The first composition is the Mg/Al composition, which matches that of the naturally occurring hydrotalcite. The second composition is Mg/Cu/Al; the third composition is Mg/Ni/Al; and the fourth composition is Mg/NiCu/Al. The study also examined the main characteristics of synthesis, the thermal disintegration of LDH, and the reformation of mixed-metal oxides into layered structures.

3. MATERIALS AND METHODS

3.1 Materials:

Magnesium nitrate hexahydrate (Mg $(NO_3)_2 \cdot 6H_2O$), aluminium nitrate nonahydrate (Al $(NO_3)_3 \cdot 9H_2O$), nickel nitrate hexahydrate (Ni $(NO_3)_2 \cdot 6H_2O$), copper nitrate trihydrate (Cu $(NO_3)_2 \cdot 3H_2O$) were utilised as the initial components in the production of LDHs in addtion Complexing agents utilised in sol-gel processing sush as monohydrates of citric acid ($C_6H_8O_7H_2O$) and ethylene glycol (CH_2OH)2 (CH_2OH). The pH was adjusted using an ammonia (NH_3) solution (All chemicals have been ordered from Merck GMBH and disectyly used without further purification).

The process of distillation was employed to purify the deionized water, which was subsequently passed through a water purification system. Additionally, all glassware utilized in the experiment was magnetically Teflon-coated.

All glassware underwent a cleaning process involving the use of distilled water, followed by ethanol washing and subsequent drying in an oven at a temperature of 150 ° C for a duration of 24 hours.

3.2 Mg3-xMx/Al1 (M = Ni, Cu) LDH Synthesis by sol-gel technique:

Table 3.1 Samples Concentrations:

LDH	Mg_g	Al_g	Ni_g	Cu_g
$Mg_{0.003}Al_{0.001}$	3	1.4630		
$MgNi_{0.0001}Al$	3	1.4630	0.1134	
$MgCu_{0.0001}Al$	3	1.4630		0.0942
MgNiCuAl	3	1.4630	0.1134	0.0942

The Mg/Ni/Cu/Al-LDH samples were synthesized by the sol–gel technique using metaftertrates $Mg(NO_3)_2 \cdot 6H_2O$, $Ni(NO_3)_2 \cdot 6H_2O$, $Cu(NO_3)_2 \cdot 3H_2O$ and $Al(NO_3)_3.9H_2O$ (3:1 molar ratio) Under continuous stirring. Stoichiometric

amounts of metals nitrate were dissolved in 50 mL of deionized water. After the addition of citric acid ($C_6H_8O_7.H_2O$, 0.2M) to the aforementioned solution, it was agitated for an hour at 80°C. Subsequently, a quantity of 2 ml of ethylene glycol $(CH_2OH)_2$ was added to the resulting mixture, which was then subjected to continuous stirring at a temperature of 150°C until the solvent was fully evaporated. Gels used in the synthesis process were dried at 105°C for 24 hours. After being ground up, the gels were heated for four hours at 650°C to produce mixed metal oxides (MMO). Deionized water was used to rehydrate the MMO powders, and the mixture was heated at 50°C for 6 hours while being constantly stirred. The final gel was dried at 70°C for 12 hours following the rehydration procedure. The MMO powders were reconstituted in water by adding ammonia to the solution, which raised the pH from 10 to 12 to create MgNiCu/Al LDH single-phase.

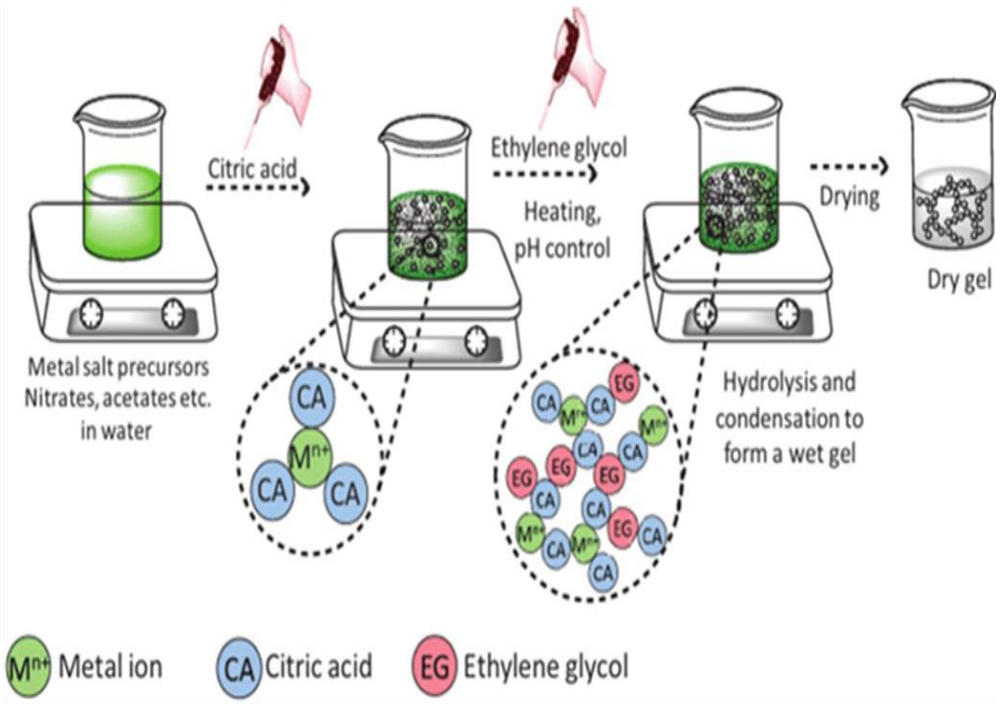

Figure 3.1 Steps in sol-gel process to achieve different final morphologies.

3.3 Characterization techniques:

Characterizing a solid substance often entails two steps: analysing its structure and measuring its properties. Structure is analysed using a wide range of microscopic as well as spectroscopic methods, while properties are characterized in a wide variety of methods. Determining the extent and method dispersing filler particles inside the matrix as well as the reaction between filler and matrix is a significant difficulty when working with nanocomposite materials. Both are crucial to the nanocomposites ability to perform their required functions. The structure and characteristics of nanocomposites have been studied using tow methods.

3.3.1 Method of X-ray Diffraction (XRD):

X-ray Powder diffraction (XRD) was taken at room temperature to examine the materials phase purity and structure. Rigaku Multiflex 2kw, power 200 vac 1Φ 30A 50Hz, diffractometers was used to capture the X-ray patterns using Cu-Ka radiation (1- 1.5418 A) at an angle range of 5-80 degrees (Picture 3.1).

Picture 3.1 Rigaku Multiflex X-Ray Diffractometer.

3.3.2 Fourier-transform infrared spectroscopy (FT-IR):

Perkin Elmer's FT-IR spectrophotometer, was used to record the infrared spectra of the final goods in the range of 4000-400 cm^{-1} (Picture 3.2). Preparation of pellets with a 0.0010:0.1500(wt/wt) KBr: product ratio yielded the product spectrum. A disc was made by pressing the sample with oven dried KBr of spectroscopic grade. Using an argon environment and a heating rate of 10 C/min, a SETARAM (SENSY-Sevo) apparatus collected thermogravimetric-differential thermal analysis (TGA-DTA) curves.

Picture 3.2 Perkin Elmer's FTIR Spectrophotometer

picture 3.2 SETARAM (SENSY-Sevo) apparatus

4. RESULTS AND DISCUSSION

4.1 Effects of Transition metals substitution in sol-gel derived $Mg_{3-x}M_x/Al_1$ (M = Ni, Cu)-LDH

The most appropriate precursors for anion exchange in LDH are those that include nitrate or chloride ions. The formation of the LDH precursor containing carbonate occurs during the sol-gel procedure (31). While the carbonate anion is a material adhesively fixed inside the interlayer galleries and usually is not subject to direct anion exchange, it is feasible to substitute it with the application of a suitable acid. This process results in the release of carbon dioxide and the integration of the acid's conjugate base (163,164).

The stoichiometric quantities of metal nitrates were dissolved in 50 mL of deionized water as well as used a teflon-lined stir bar was placed in the flask (100ml) and the flask was positioned on a magnetic stirrer (Heidolph MR301). Following the addition of citric acid ($C_6H_8O_7.H_2O$, 0.2M) into the previously described solution, the mixture was subjected to agitation for one hour under a temperature of 80°C. Following this, 2 ml of ethylene glycol was added to the resultant mixture, which was then exposed to continuous agitation at a temperature of 150°C until complete evaporation of the solvent occurred. In this step of the procedure, a colloidal solution is generated by the process of mechanically mixing colloidal particles inside a water based as solvent. The metal alkoxide precursor $M(OR)_4$ undergoes hydrolysis and polycondensation reactions upon reacting with water. This results in the creation of a colloidal dispersion consisting of particles with sizes ranging from 1 to 2 nm. Eventually, these particles experience further transformations and convert into a three-dimensional network composed of the inorganic oxide of corresponding. The usage of ethylene glycol as a stabilising ingredient serves to enhance polymerization, hence promoting homogeneity. The primary function of citric acid is to facilitate the formation of a polymeric network via condensation processes, whereby it establishes three-bond connections with the metal cation.

Chelating substances, such as citric acid as well as ethylene glycol, inhibit the mobility of metallic ions within a solution and hinder the partial separation of cations in the end compound. This effect is achieved by a reaction between the metallic ions. The addition of ethylene glycol below heat effect, will result in the polyesterification process of the chelates causing the establishment of a three-dimensional interconnected structure composed of organic radicals and metal atoms. The gels used in the synthesis procedure were submited to a drying process at a temperature of 105°C for a duration of 24 hours. The liquid phase that was initially present inside the gel matrix underwent a gradual evaporation process under ambient temperatures resulting in the formation of a brittle solid material known as xerogel.

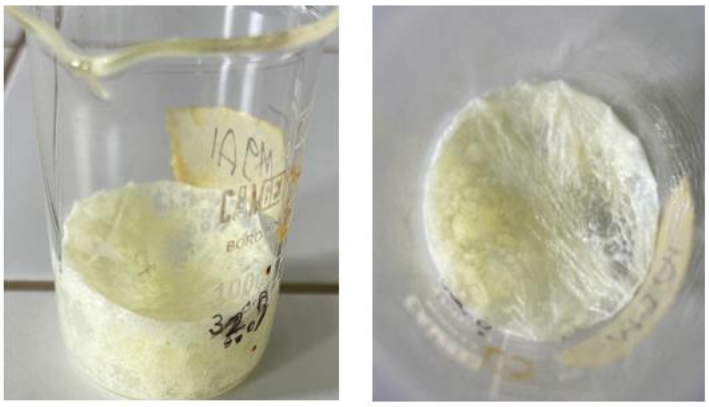

Figure 4.1 The dried gel of $Mg_{0.003}/Al_{0.001}$ obtained after heated at 105°C for 24H

Figure 4.2 The dried gel of $Mg_{0.003}/Cu_{0.0001}/Al_{0.001}$ obtained after heated at 105°C for 24H

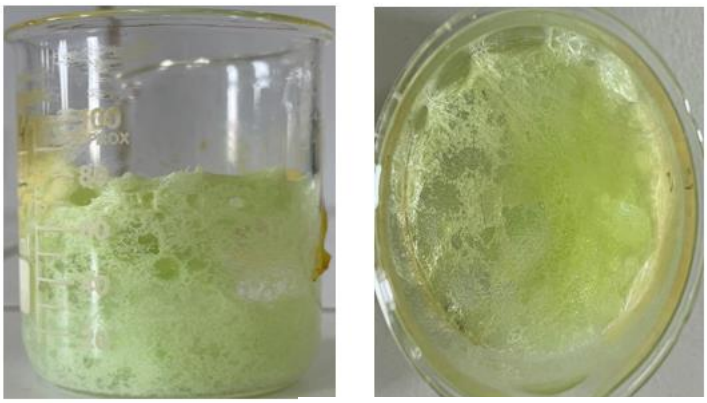

Figure 4.3 The dried gel of $Mg_{0.003}/Ni_{0.0001}/Al_{0.001}$ obtained after heated at 105˚C for 24H

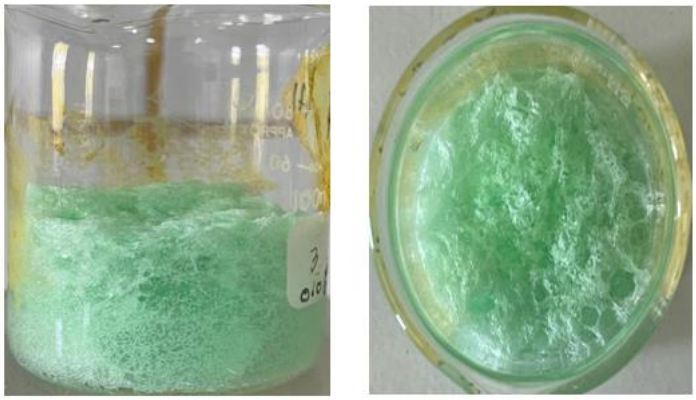

Figure 4.4 The dried gel of $Mg_{0.003}/Ni_{0.0001}/Cu_{0.0001}/Al_{0.001}$ obtained after heated at 105˚C for 24H

During the end phase of the synthesis process, the sol-gel method includes a step known as Ageing, which is sometimes referred to as Syneresis. It consists of keeping the cast object in good condition for a while, which might be a few hours or several days. During the process of aging, polycondensation persists in conjunction with the surrounding solution, leading to the reprecipitation of the gel network. This procedure will result in an augmentation of the interparticle necks thickness and a reduction in porosity. Therefore, the efficancy of the gel is enhanced by this phenomenon, resulting in the creation of a product that exhibits resistance to cracking during the drying process.

To a dense, pore-free, and homogenous material from the xerogel, it is necessary to undergo a sintering process. The approach represents the conventional methodology for acquiring a bulk of material that may be subsequently processed to provide sol-gel particles suitable for various applications. The gels underwent a grinding process and were then subjected to a four-hour heating treatment at a temperature of 650°C, resulting in the formation of mixed metal oxides (MMO).

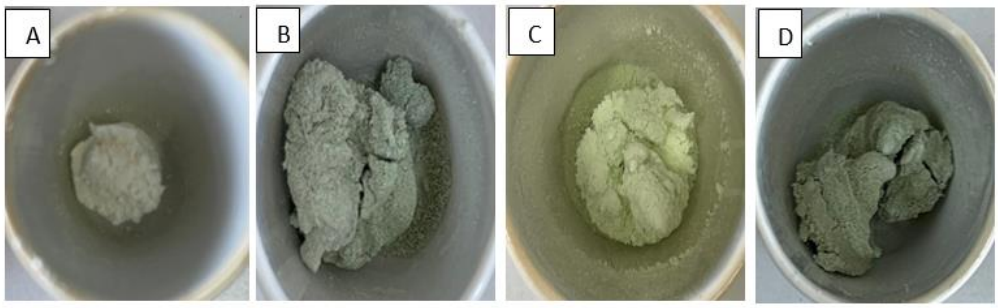

Figure 4.5 A) MgAl, **B)** MgCuAl, **C)** MgNiAl, **D)** MgCuNiAl obtained after heated 650 C°mix metal oxides (MMO).

Deionized water was used for the purpose of rehydrating the MMO powders. The resulting mixture was subjected to continuous stirring and heated to a temperature of 50°C for 6 hours. The ultimate gel underwent a desiccation process at a temperature of 70°C for 12 hours after the rehydration step.

During the drying phase, the complex network undergoes solvent removal to eliminate any surplus. During the process of drying, significant capillary strains may arise in situations where the size of the pores is quite small. The application of stress induces instantaneous cracking in the gels, which can only be mitigated by controlling the process by a reduction in the liquid surface area.

This may be achieved by the process of hypercritical evaporation, wherein the solid and liquid components are prevented from interacting.

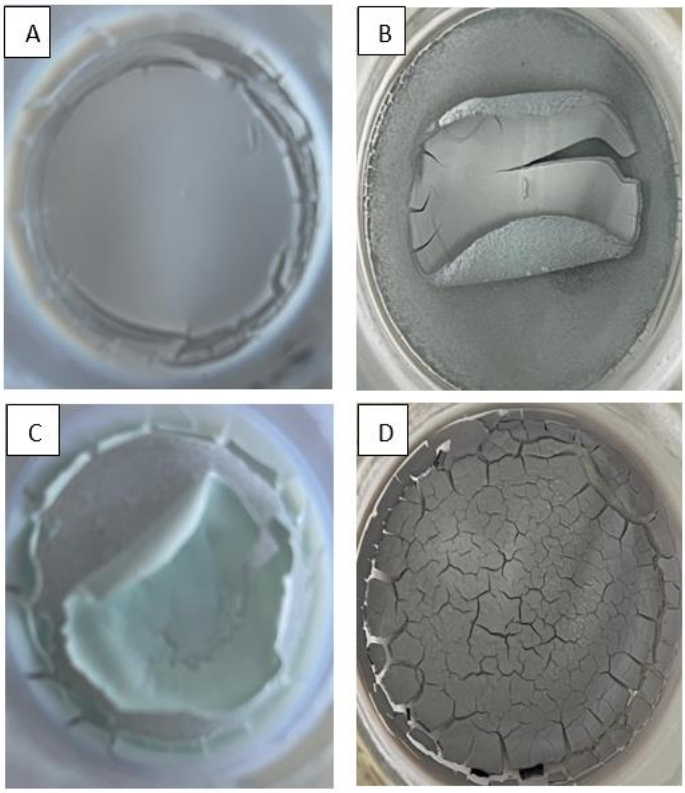

Figure 4.6 A) MgAl, **B)** MgCuAl, **C)** MgNiAl, **D)** MgCuNiAl obtained after heated at 70˚C for 12H.

4.2 Examination of phase purity and crystal structure:

The X-ray diffraction (XRD) patterns illustrating the mixed metal oxides formed from the precursor gels of Mg_2/Al_1-(LDHs) during heating samples are shown in Fig. 4.7 obtained from four samples subjected to a temperature at 650 ºC exhibited two distinct XRD peaks. These peaks indicate the presence of a mixed metal oxide (MMO) phase, which has a structure like that of magnesium oxide (JCPDS No. 96-100-0054) (31). In every case, weakly crystalline magnesium oxide is formed. However, the MgCuNiAl-containing samples' XRD patterns also showed reflections of a NiO and CuO phase.

The treatment of heat to a layered double hydroxide at high temperatures leads to the removal of interlayer water molecules located between the layers, and the loss of anions that were there to maintain charge balance. resulting in the removal of hydroxyl groups from the brucite-like layers.

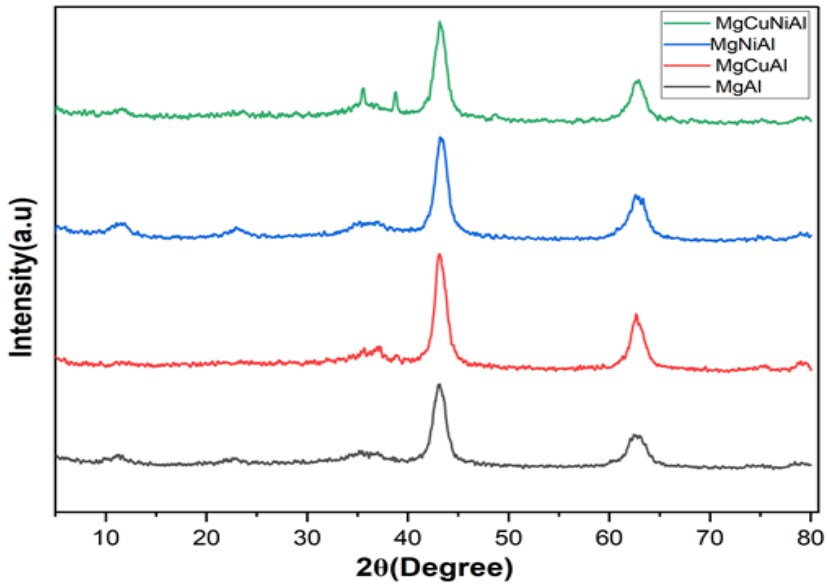

Figure 4.7 The X-ray diffraction (XRD) for the mixed metal oxides (MMO)

Fig. 4.8 displays the (XRD) patterns of four different layered double hydroxide samples: MgAl-LDH, MgCuAl-LDH, MgNiAl-LDH, and MgNiCuAl-LDH before to adjusting the pH of the samples to pH12.

The (XRD) patterns of all four samples had a high degree of similarity, indicating that they shared comparable structural characteristics. Additionally, the diffraction peaks seen in the XRD patterns were consistent with those often observed in layered double hydroxide materials. The presence of well-defined peaks in the Mg-Al-NO_3 LDH sample can be seen, and these peaks may be ascribed to hydrotalcite (JCPDS No. 20-0700). This indicates that the sample has a layered double hydroxide structure with varying amounts of metal substitution. Distinctive diffraction peaks corresponding to the LDH structure were seen at approximate 2θ angles of 11.46º (003), 22.85º (006), and 34.5º (009) (165). Furthermore, it is worth noting that two supplementary LDH peaks were clearly seen at about 60.61º and 61.92º, which may be attributed to the reflections originating from the (110) and (113) crystallographic planes (31). The reflections (015) and (018) Less important (166), which are seen at around 38-93° and 46-24°, respectively, are likewise associated with the LDH phase. Based on the

analysis of the primary reflections (003) and (006), it can be shown that the LDHs doped with MgAl- and MgCuAl exhibit greater crystallinity compared to those containing MgNiAl and MgCuNiAl under identical reaction conditions. Furethemore, The MgCuAl sample has a distinct structural composition when compared with the other samples, characterized by the presence of a predominant crystalline phase known as CuO. According to the solubility curves and predominance diagrams pertaining to Cu^{2+} ions, it can be shown that at a very alkaline pH, the solubility of copper-hydroxy complexes, namely hydrotalcite, increases, whereas the predominant phase that would precipitate is CuO. The present study determines that the formation of the hydrotalcite phase at a lower pH during the synthesis process leads to its subsequent dissolution at a higher pH, resulting in the formation of CuO (167).

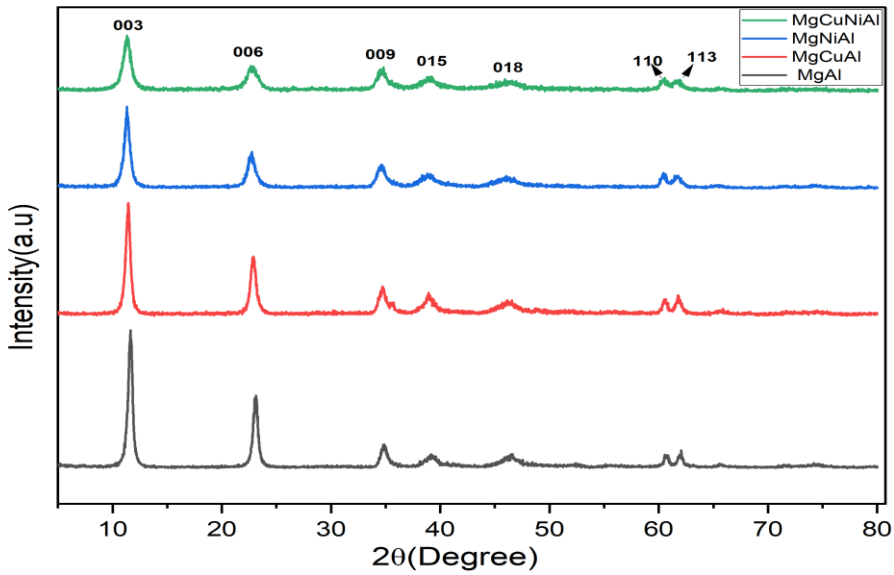

Figure 4.8 The X-ray diffraction (XRD) for the layered double hydroxide (LDH) before pH12.

Fig 4.9 illustrates the influence of pH on the preparation of Magnesium-Aluminum Nitrate Layered Double Hydroxides (Mg-Al–NO_3–LDHs), The pH of the preparation plays a crucial role in the creation of hydrotalcite-type materials with the optimal pH being dependent on the specific cations used.

The samples that were synthesized within the pH range of pH12 exhibit patterns that are comparable to those seen in natural hydrotalcite (155). The formation of the hydrotalcite phase, accompanied by the presence of an extra NH_3 phase, occurs in alkaline conditions with a pH of 12. The observed distinction among these samples lies in the varying intensities of the (001) reflections. In these patterns, the intensity of the reflections exhibits an upward trend, while the line width shows a reduction, these changes are indicative of an enhanced level of high crystallinity.

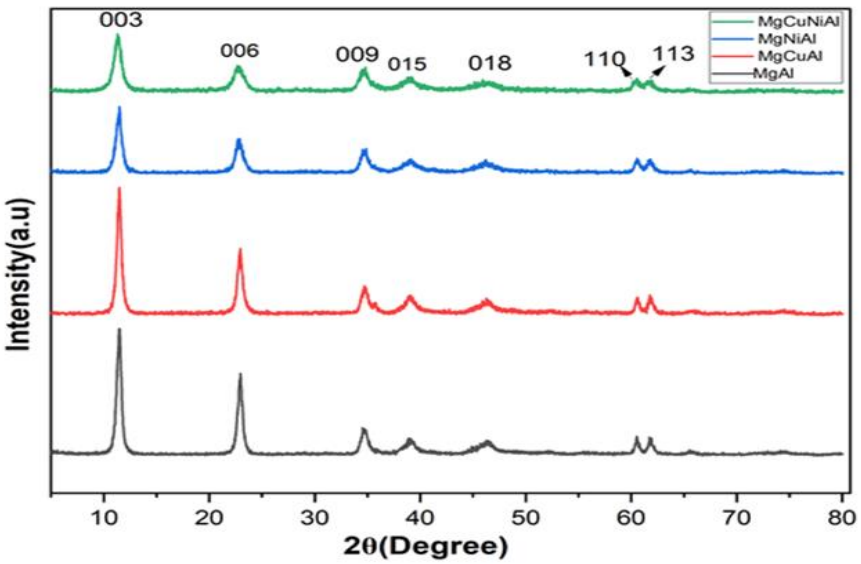

Figure 4.9 The X-ray diffraction (XRD) for the layered double hydroxide (LDH) after pH12.

4.3 FT-IR Spectroscopic Analysis

Fig 4.10 displays the FT-IR spectra of the synthesised magnesium hydroxide ($Mg(OH)_2$) and calcined magnesium oxide (MgO) nanoparticles. The phenomenon of chemisorption of H_2O and CO_2 molecules onto the surface of MgO when exposed to the environment is well known. The spectra of the calcined sample exhibit a strong vibration band at 3450 cm^{-1}, which may be attributed to the OH stretching vibrations of water molecules that are adsorbed on the surface (168). Additionally, the bands seen at 1636 cm^{-1} are indicative of the bending vibrations of the same surface-adsorbed water molecules (169). Furthermore, there is a discernible band of low intensity that corresponds to the adsorption of gaseous CO_2 at 2426 cm^{-1} (170), whereas the existence of NO_3^- peak is shown at 1384 cm^{-1} (171). The observed bands at the low frequencies in the range of 470 – 480 cm^{-1} could be ascribed to the stretching vibrations associated with the bonding between magnesium (Mg) and oxygen (O) atoms in the Mg-O-Mg structure (172).

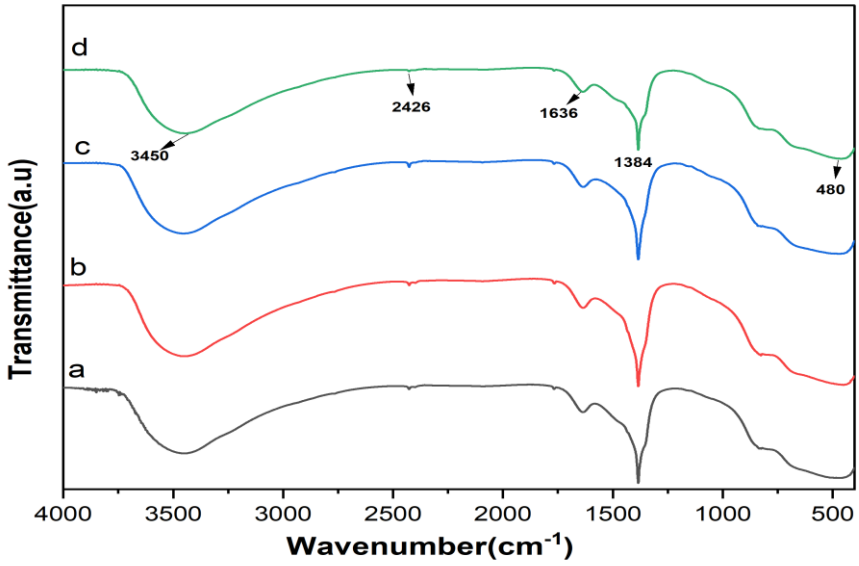

Figure 4.10 FT-IR spectra for **a)** MgAl, **b)** MgCuAl **c)** MgNiAl, **d)** MgCuNiAl-the mixed metal oxides (MMO).

In the FT-IR spectra of all Mg-Al LDH-NO_3^- samples, the distinctive absorption peak at 1383 cm^{-1} is identified to the NO_3^- group (171). The observed intense and narrow absorption peak is ascribed to the ν_3 vibrational manner, which exhibits D3h symmetry in the NO_3^- structure. The appearance of the prominent sharp and strong peak at 412 cm^{-1} in several FT-IR spectra of Mg-Al LDH-NO_3 (172). This vibration band could be attributed to the stretching vibration of metal-oxygen bonds inside the brucite-like lattice structure. In the next two fig displays the Fourier Transform Infrared (FT-IR) spectrum of Mg-Al (LDH)- NO_3^-, which was synthesised via the sol-gel technique utilising aluminum and magnesium nitrate. The absorption band seen at a central wavenumber of 3545 cm^{-1} was designated to the stretching vibration of the O-H bond in the metal-hydroxide layer and the water molecules present between the layers (168).

The water interlayer's bending vibration displayed a reflection peak at a wavenumber of 1647 cm^{-1} (169). Furthermore, the stretching vibration of NO_3 was seen at a wavenumber of 1383 cm^{-1}. The observed absorption bands within the spectral range of 557-663 cm^{-1} were ascribed to the stretching manner of Al-O and Mg-O.

In general, an increase in pH during the synthesis conditions leads to a corresponding increase in the intensity of the infrared bands. Given that there is a direct relationship between intensity and order, it can be inferred that the samples synthesised at pH level 12 exhibit the highest degree of crystallinity, while the sample generated at pH 8 has the lowest degree of crystallinity.

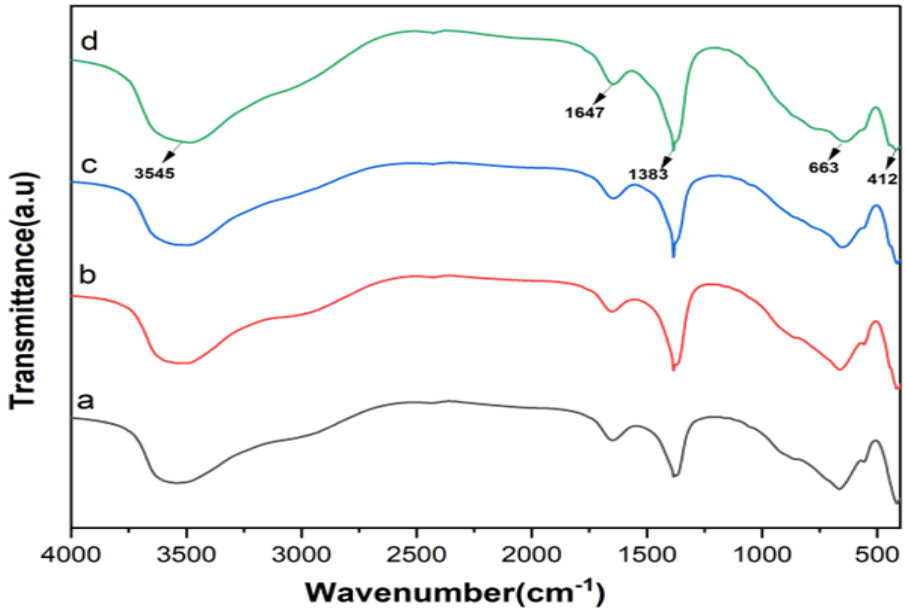

Figure 4.11 FT-IR spectra for **a)** MgAl, **b)** MgCuAl **c)** MgNiAl, **d)** MgCuNiAl the layered double hydroxide (LDH) before pH.

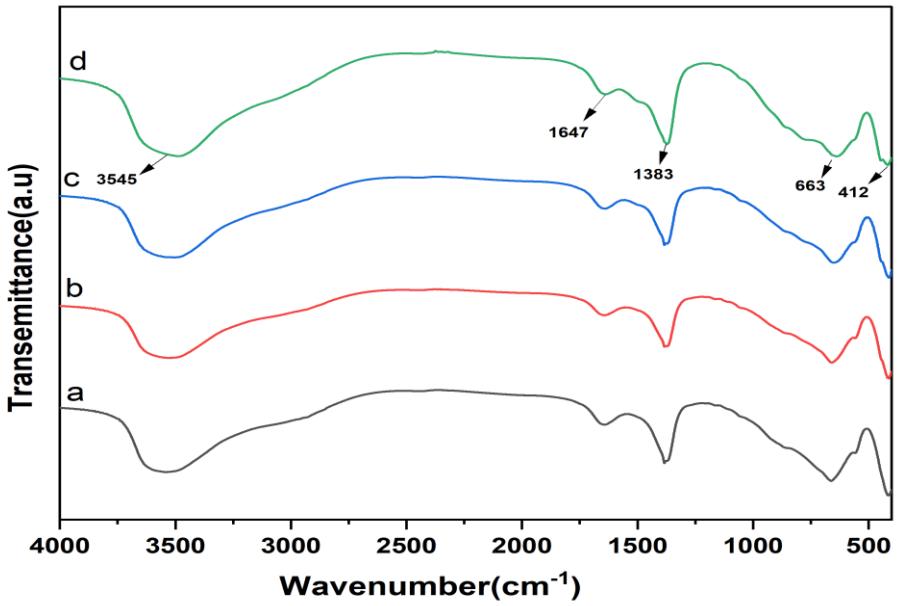

Figure 4.12 FT-IR spectra for **a)** MgAl, **b)** MgCuAl **c)** MgNiAl, **d)** MgCuNiAl the layered double hydroxide (LDH) after pH12.

5. CONCLUSIONS

1. The $Mg_{3-x}M_x/Al_1$ (M =Ni, Cu) (LDHs) were effectively synthesised using an aqueous sol-gel technique. The process included the transformation of mixed metal oxides into layered double hydroxides using either water or a solution of magnesium nitrate.

2. To produce the LDHs, the precursor gels were decomposed (calcinated) at 650 °C, and then the resulting crystalline MMO powders were rehydrated in water.

3. The parameter of aging time has significance in the regulation of crystallinity as well as particle size. Empirical investigations have shown that a duration of 12 hours is adequately sufficient to get a well-crystallized phase of hydrotalcite.

4. The experimental findings revealed that the introduction of varying amounts of Ni and Cu into the sol-gel-derived layered double hydroxides (LDHs) did not result in the destruction of their layered structure. furthermore, copper and nickel could be replaced in the magnesium locations in the Mg_3Al_1 LDHs without the formation of impurities.

5. Surface characteristics and porosity of final products were shown to be influenced by the kind and concentration of transition metal used.

6. The results of the experiments showed that at pH 12, a pure phase of hydrotalcite may be generated, indicating that pH plays an important factor in the synthesis of M-Al hydrotalcite-type materials.

7. The sol-gel synthesis technique suggested for layered double hydroxides (LDHs) has many advantages compared to traditional approaches. These include its simplicity, which allows for ease of implementation, as well as the high homogeneity of the final products. Additionally, the sol-gel method proves to be successful in producing LDHs and is suitable for studying substitution effects in various multinary metal systems. Moreover, this synthesis pathway is cost-efficient.

8. The X-ray diffraction (XRD) pattern of the mixed metal oxide (MMO) sample, which was produced by subjecting precursor gels containing Mg-Al-O to a temperature of 650 ◦C, revealed the existence of one phase of MMO.

The study revealed that the microstructure of the rebuilt mixed metal oxide (MMO) acquired from sol-gel generated layered double hydroxides (LDHs) exhibited a phenomenon referred to as the "memory effect." This effect implies

that the microstructural characteristics of the MMO closely resembled those established for the LDHs.

9. The Fourier Transform Infrared (FTIR) findings obtained in this work provided comprehensive support for the X-ray Diffraction (XRD) analytical data and confirmed the excellent repeatability of the sol-gel processing technique utilised for the synthesis of mixed-metal Layered Double Hydroxide (LDH) samples.

6. REFERENCES

"Vancouver citation system was used in this thesis."

1. Heiligtag FJ, Niederberger M. The fascinating world of nanoparticle research. Mater Today [Internet]. 2013;16(7):262–71. Available from: https://www.sciencedirect.com/science/article/pii/S1369702113002253

2. De M, Ghosh PS, Rotello VM. Applications of Nanoparticles in Biology. Adv Mater [Internet]. 2008 Nov 18;20(22):4225–41. Available from: https://doi.org/10.1002/adma.200703183

3. Cavani F, Trifirò F, Vaccari A. Hydrotalcite-type anionic clays: Preparation, properties and applications. Catal Today. 1991;11(2):173–301.

4. Lagaly G. GENERAL INTRODUCTION : CLAYS , CLAY MINERALS , AND CLAY SCIENCE. 2006;1(05).

5. Bergaya F, Lagaly G. General introduction: clays, clay minerals, and clay science. Dev clay Sci. 2006;1:1–18.

6. Evans DG, Slade RCT. Structural aspects of layered double hydroxides. Layer double hydroxides. 2006;1–87.

7. Forano C, Hibino T, Leroux F, Taviot-Gueho C. Handbook of Clay Science Developments in Clay Science. In: Layered Double Hydroxides. Elsevier Ltd; 2006. p. 1021–95.

8. De Roy A. Layered double hydroxides. Springer Science & Business Media. 2006.

9. Fernandez JM, Barriga C, Ulibarri MA, Labajos FM, Rives VJ. Kagunya W, Hassan Z, Jones W. Inorg Chem. 1996;35:5970.

10. Carlino S. Chemistry between the sheets. Chem Br. 1997;33(9):59–62.

11. Bröcker FJ, Kainer L. German Patent, 2024282, 1970. UK Pat. 1971;1342020.

12. Zelinsky N, Kommarewsky W. Über die katalytischen Wirkungen des nickelierten Tonerde-Hydrats. Berichte der Dtsch Chem Gesellschaft (A B Ser. 1924;57(4):667–9.

13. Reichle WT. Synthesis of anionic clay minerals (mixed metal hydroxides, hydrotalcite). Solid State Ionics. 1986;22(1):135–41.

14. Carrado KA, Kostapapas A, Suib SL. Layered double hydroxides (LDHs). Solid State Ionics. 1988;26(2):77–86.

15. Allmann R. The crystal structure of pyroaurite. Acta Crystallogr Sect B Struct Crystallogr Cryst Chem. 1968;24(7):972–7.

16. Taylor HFW. Mineral. Mag. 1973.

17. Lee JH, Jung D-Y, Kim E, Ahn TK. Fluorescein dye intercalated layered double hydroxides for chemically stabilized photoluminescent indicators on inorganic surfaces. Dalt Trans. 2014;43(22):8543–8.

18. Chen Y, Jing C, Zhang X, Jiang D, Liu X, Dong B, et al. Acid-salt treated CoAl layered double hydroxide nanosheets with enhanced adsorption capacity of methyl orange dye. J Colloid Interface Sci [Internet]. 2019;548:100–9. Available from: https://www.sciencedirect.com/science/article/pii/S0021979719304138

19. Varadwaj GBB, Oyetade OA, Rana S, Martincigh BS, Jonnalagadda SB, Nyamori VO. Facile synthesis of three-dimensional Mg–Al layered double hydroxide/partially reduced

graphene oxide nanocomposites for the effective removal of Pb2+ from aqueous solution. ACS Appl Mater Interfaces. 2017;9(20):17290–305.

20. Rao C, Müller A, Cheetham A. The chemistry of nanomaterials: synthesis, properties and applications. John Wiley & Sons. 2006.

21. Tonelli D, Scavetta E, Giorgetti M. Layered-double-hydroxide-modified electrodes: electroanalytical applications. Anal Bioanal Chem. 2013;405:603–14.

22. Chisem IC, Jones W. Ion-exchange properties of lithium aluminium layered double hydroxides. J Mater Chem. 1994;4(11):1737–44.

23. Gupta S, Agarwal DD, Banerjee S. Lithium aluminium layered double hydroxides: synthesis and application in poly (vinyl chloride). Int J Polym Mater. 2012;61(13):985–98.

24. Tichit D, Das N, Coq B, Durand R. Preparation of Zr-containing layered double hydroxides and characterization of the acido-basic properties of their mixed oxides. Chem Mater. 2002;14(4):1530–8.

25. Chaparadza A, Hossenlopp JM. Removal of 2, 4-dichlorophenoxyacetic acid by calcined Zn–Al–Zr layered double hydroxide. J Colloid Interface Sci. 2011;363(1):92–7.

26. Velu S, Suzuki K, Osaki T, Ohashi F, Tomura S. Synthesis of new Sn incorporated layered double hydroxides and their evolution to mixed oxides. Mater Res Bull. 1999;34(10–11):1707–17.

27. Xia S-J, Liu F-X, Ni Z-M, Shi W, Xue J-L, Qian P-P. Ti-based layered double hydroxides: efficient photocatalysts for azo dyes degradation under visible light. Appl Catal B Environ. 2014;144:570–9.

28. De Roy A, Forano C, Besse JP. Layered double hydroxides: synthesis and post-synthesis modification. Layer double hydroxides Present Futur. 2001;1–39.

29. Valente JS, Figueras F, Gravelle M, Kumbhar P, Lopez J, Besse J-P. Basic properties of the mixed oxides obtained by thermal decomposition of hydrotalcites containing different metallic compositions. J Catal. 2000;189(2):370–81.

30. Millange F, Walton RI, O'Hare D. Time-resolved in situ X-ray diffraction study of the liquid-phase reconstruction of Mg–Al–carbonate hydrotalcite-like compounds. J Mater Chem. 2000;10(7):1713–20.

31. Smalenskaite A, Vieira DEL, Salak AN, Ferreira MGS, Katelnikovas A, Kareiva A. A comparative study of co-precipitation and sol-gel synthetic approaches to fabricate cerium-substituted MgAl layered double hydroxides with luminescence properties. Appl Clay Sci. 2017;143:175–83.

32. Sokol D, Salak AN, Ferreira MGS, Beganskiene A, Kareiva A. Bi-substituted Mg3Al–CO3 layered double hydroxides. J Sol-Gel Sci Technol [Internet]. 2018;85(1):221–30. Available from: https://doi.org/10.1007/s10971-017-4506-9

33. Seiyama T, Yamazoe N, Eguchi K. Characterization and activity of some mixed metal oxide catalysts. Ind Eng Chem Prod Res Dev. 1985;24(1):19–27.

34. Védrine JC. Heterogeneous catalysis on metal oxides. Catalysts. 2017;7(11):341.

35. Velu S, Suzuki K, Gopinath CS. Photoemission and in situ XRD investigations on CuCoZnAl-mixed metal oxide catalysts for the oxidative steam reforming of methanol. J Phys Chem B. 2002;106(49):12737–46.

36. Cho S, Jang J, Kong K, Kim ES, Lee K, Lee JS. Anion-doped mixed metal oxide nanostructures derived from layered double hydroxide as visible light photocatalysts. Adv Funct Mater. 2013;23(19):2348–56.

37. Hu W, Wei H, She Y, Tang X, Zhou M, Zang Z, et al. Flower-like nickel-zinc-cobalt mixed metal oxide nanowire arrays for electrochemical capacitor applications. J Alloys Compd. 2017;708:146–53.

38. Miura N, Lu G, Yamazoe N. High-temperature potentiometric/amperometric NOx sensors combining stabilized zirconia with mixed-metal oxide electrode. Sensors Actuators B Chem. 1998;52(1–2):169–78.

39. Paul D, Neogi S. Synthesis, characterization and a comparative antibacterial study of CuO, NiO and CuO-NiO mixed metal oxide. Mater Res Express. 2019;6(5):55004.

40. Wang Y, Zhang D, Lv D, Sun Y. Mg–Al mixed metal oxide film derived from layered double hydroxide precursor film: fabrication and antibacterial properties. J Taiwan Inst Chem Eng. 2015;57:160–6.

41. Polychronopoulou K, Fierro JLG, Efstathiou AM. Novel Zn–Ti-based mixed metal oxides for low-temperature adsorption of H2S from industrial gas streams. Appl Catal B Environ. 2005;57(2):125–37.

42. Zhang Z, Liao M, Zeng H-Y, Xu S, Liu X, Du J, et al. Temperature effect on chromium (VI) removal by Mg/Al mixed metal oxides as adsorbents. Appl Clay Sci. 2014;102:246–53.

43. Ni Z-M, Xia S-J, Wang L-G, Xing F-F, Pan G-X. Treatment of methyl orange by calcined layered double hydroxides in aqueous solution: adsorption property and kinetic studies. J Colloid Interface Sci. 2007;316(2):284–91.

44. Jiang D, Su L, Ma L, Yao N, Xu X, Tang H, et al. Cu–Zn–Al mixed metal oxides derived from hydroxycarbonate precursors for H2S removal at low temperature. Appl Surf Sci. 2010;256(10):3216–23.

45. Lee S-B, Ko E-H, Park JY, Oh J-M. Mixed metal oxide by calcination of layered double hydroxide: Parameters affecting specific surface area. Nanomaterials. 2021;11(5):1153.

46. Zhao M-Q, Zhang Q, Zhang W, Huang J-Q, Zhang Y, Su DS, et al. Embedded high density metal nanoparticles with extraordinary thermal stability derived from guest− host mediated layered double hydroxides. J Am Chem Soc. 2010;132(42):14739–41.

47. Hibino T. Layered double hydroxide–agarose composites for water treatment: Carbonate contamination during the drying process. Appl Clay Sci. 2015;116:93–101.

48. Daza CE, Cabrera CR, Moreno S, Molina R. Syngas production from CO2 reforming of methane using Ce-doped Ni-catalysts obtained from hydrotalcites by reconstruction method. Appl Catal A Gen. 2010;378(2):125–33.

49. Takehira K. Recent development of layered double hydroxide-derived catalysts− Rehydration, reconstitution, and supporting, aiming at commercial application−. Appl Clay Sci. 2017;136:112–41.

50. Abdelsadek Z, Sehailia M, Halliche D, Gonzalez-Delacruz VM, Holgado JP, Bachari K, et al. In-situ hydrogasification/regeneration of NiAl-hydrotalcite derived catalyst in the reaction of CO2 reforming of methane: A versatile approach to catalyst recycling. J CO2 Util. 2016;14:98–105.

51. Muñoz M, Morceno S, Molina R. Synthesis of Ce and Pr-promoted Ni and Co catalysts from hydrotalcite type precursors by reconstruction method. Int J Hydrogen Energy. 2012;37(24):18827–42.

52. Tanasoi S, Tanchoux N, Urdă A, Tichit D, Săndulescu I, Fajula F, et al. New Cu-based mixed oxides obtained from LDH precursors, catalysts for methane total oxidation. Appl Catal A Gen. 2009;363(1–2):135–42.

53. Basile F, Benito P, Fornasari G, Vaccari A. Hydrotalcite-type precursors of active catalysts for hydrogen production. Appl Clay Sci. 2010;48(1–2):250–9.

54. Sikander U, Sufian S, Salam MA. ScienceDirect A review of hydrotalcite based catalysts for hydrogen production systems. Int J Hydrogen Energy [Internet]. 2017;42(31):19851–68. Available from: http://dx.doi.org/10.1016/j.ijhydene.2017.06.089

55. Hora L, Kikhtyanin O, Čapek L, Bortnovskiy O, Kubička D. Comparative study of physico-chemical properties of laboratory and industrially prepared layered double hydroxides and their behavior in aldol condensation of furfural and acetone. Catal Today. 2015;241:221–30.

56. Kalai DY, Stangeland K, Jin Y, Tucho WM, Yu Z. Biogas dry reforming for syngas production on La promoted hydrotalcite-derived Ni catalysts. Int J Hydrogen Energy. 2018;43(42):19438–50.

57. Lino AVP, Assaf EM, Assaf JM. Hydrotalcites derived catalysts for syngas production from biogas reforming: Effect of nickel and cerium load. Catal Today. 2017;289:78–88.

58. Liu H, Wierzbicki D, Debek R, Motak M, Grzybek T, Da Costa P, et al. La-promoted Ni-hydrotalcite-derived catalysts for dry reforming of methane at low temperatures. Fuel. 2016;182:8–16.

59. Perez-Lopez OW, Senger A, Marcilio NR, Lansarin MA. Effect of composition and thermal pretreatment on properties of Ni–Mg–Al catalysts for CO2 reforming of methane. Appl Catal A Gen. 2006;303(2):234–44.

60. Tang S, Yao Y, Chen T, Kong D, Shen W, Lee HK. Recent advances in the application of layered double hydroxides in analytical chemistry: A review. Anal Chim Acta. 2020;1103:32–48.

61. Burns A, Ow H, Wiesner U. Fluorescent core–shell silica nanoparticles: Towards “Lab on a Particle” architectures for nanobiotechnology. Chem Soc Rev. 2006;35(11):1028–42.

62. Miyata S. The Syntheses of Hydrotalcite-Like Compounds and Their Structures and Physico-Chemical Properties—I: the Systems Mg2+-Al3+-NO3−, Mg2+-Al3+-Cl−, Mg2+-Al3+-ClO4−, Ni2+-Al3+-Cl− and Zn2+-Al3+-Cl−. Clays Clay Miner [Internet]. 1975;23(5):369–75. Available from: https://doi.org/10.1346/CCMN.1975.0230508

63. Cavani F, Trifiro F, Vaccari A. Hydrotalcite-type anionic clays: Preparation, properties and applications. Catal today. 1991;11(2):173–301.

64. Shirin VKA, Sankar R, Johnson AP, Gangadharappa H V, Pramod K. Advanced drug delivery applications of layered double hydroxide. J Control Release. 2021;330:398–426.

65. Taviot-Guého C, Prévot V, Forano C, Renaudin G, Mousty C, Leroux F. Tailoring hybrid layered double hydroxides for the development of innovative applications. Adv Funct Mater. 2018;28(27):1703868.

66. Zümreoglu-Karan B, Ay A. Layered double hydroxides—multifunctional nanomaterials. Chem Pap. 2012;66(1):1–10.

67. Khan A. Intercalation chemistry of layered double hydroxides: recent developments and applicationsBasis of a presentation given at Materials Discussion No. 5, 22???25 September 2002, Madrid, Spain. J Mater Chem - J MATER CHEM. 2002 Oct 24;12:3191–8.

68. Newman SP, Jones W. Synthesis, characterization and applications of layered double hydroxides containing organic guests. New J Chem. 1998;22(2):105–15.

69. Jaubertie C, Holgado MJ, San Román MS, Rives V. Structural characterization and delamination of lactate-intercalated Zn, Al-layered double hydroxides. Chem Mater.

2006;18(13):3114–21.

70. Miyata S. Anion-exchange properties of hydrotalcite-like compounds. Clays Clay Miner. 1983;31:305–11.

71. Wang Q, O'Hare D. Recent advances in the synthesis and application of layered double hydroxide (LDH) nanosheets. Chem Rev. 2012;112(7):4124–55.

72. Hu G, Wang N, O'Hare D, Davis J. Synthesis of magnesium aluminium layered double hydroxides in reverse microemulsions. J Mater Chem [Internet]. 2007;17(21):2257–66. Available from: http://dx.doi.org/10.1039/B700305F

73. Hu G, Wang N, O'Hare D, Davis J. One-step synthesis and AFM imaging of hydrophobic LDH monolayers. Chem Commun. 2006;(3):287–9.

74. Adachi-Pagano M, Forano C, Besse J-P. Delamination of layered double hydroxides by use of surfactants. Chem Commun. 2000;(1):91–2.

75. O'Leary S, O'Hare D, Seeley G. Delamination of layered double hydroxides in polar monomers: new LDH-acrylate nanocomposites. Chem Commun. 2002;(14):1506–7.

76. Hibino T, Jones W. New approach to the delamination of layered double hydroxides. J Mater Chem. 2001;11(5):1321–3.

77. Zhao W, Gu J, Zhang L, Chen H, Shi J. Fabrication of uniform magnetic nanocomposite spheres with a magnetic core/mesoporous silica shell structure. J Am Chem Soc. 2005 Jun;127(25):8916–7.

78. Wypych F, Bubniak GA, Halma M, Nakagaki S. Exfoliation and immobilization of anionic iron porphyrin in layered double hydroxides. J Colloid Interface Sci. 2003;264(1):203–7.

79. Xu ZP, Braterman PS. Layered Double Hydroxides: Self-Assembly and Multiple Phases. Marcel Dekker Inc., New York; 2004.

80. Labajos FM, Rives V, Ulibarri MA. A FT-IR and V-UV Spectroscopic Study of Nickel-Containing Hydrotalcite-Like Compounds,[Ni1− xAlx (OH) 2](CO3) x/2. nH2O. Spectrosc Lett. 1991;24(4):499–508.

81. Xu Z, Zeng H. Abrupt Structural Transformation in Hydrotalcite-like Compounds Mg 1- x Al x (OH) 2 (NO 3) x · n H 2 O as a Continuous Function of Nitrate Anions. J Phys Chem B - J PHYS CHEM B. 2001 Mar 1;105:1743–9.

82. Hofmeister W, Platen H Von. Crystal chemistry and atomic order in brucite-related double-layer structures. Crystallogr Rev. 1992;3(1):3–26.

83. Miyata S, Kumura T. Synthesis of new hydrotalcite-like compounds and their physico-chemical properties. Chem Lett. 1973;2(8):843–8.

84. Chibwe K, Valim JB, Jones W. The synthesis and catalytic applications of layered double hydroxides. Prepr Chem Soc Div Pet Chem. 1989;34(3):507–10.

85. Taylor HFW. Crystal structures of some double hydroxide minerals. Mineral Mag. 1973;39(304):377–89.

86. Allmann R, Lohse HH. Die Kristallstruktur des Sjögrenits und eines Umwandlungsproduktes des Koenenits. N Jahrb Miner Mh. 1966;6:161–81.

87. Peterson RC, Hill RJ, Gibbs G V. A molecular-orbital study of distortions in the layer structures brucite, gibbsite and serpentine. Can Mineral. 1979;17(4):703–11.

88. Koritnig S, Süsse P. Meixnerit, Mg6Al2(OH)18·4H2O, ein neues Magnesium-Aluminium-Hydroxid-Mineral. Tschermaks Mineral und Petrogr Mitteilungen [Internet].

1975;22(1):79–87. Available from: https://doi.org/10.1007/BF01081303

89. Bish DL. Anion-exchange in takovite: applications to other hydroxide minerals. Bull Mineral. 1980;103(2):170–5.

90. Willems van den W. Roadmap report on nanoparticles. W&W Espana sl, Barcelona, Spain. 2005;157.

91. Hen Y, Chen H, Zeng D, TiaCn Y, Chen F, Feng J, et al. Core/shell structured hollow mesoporous nanocapsules: A potential platform for simultaneous cell imaging and anticancer drug delivery. ACS Nano. 2010;4(10):6001–13.

92. Wei S, Wang Q, Zhu J, Sun L, Lin H, Guo Z. Multifunctional composite core-shell nanoparticles. Nanoscale. 2011;3(11):4474–502.

93. Li C, Ma C, Wang F, Xi Z, Wang Z, Deng Y, et al. Preparation and biomedical applications of core-shell silica/magnetic nanoparticle composites. J Nanosci Nanotechnol. 2012;12(4):2964–72.

94. Long NV, Yang Y, Minh Thi C, Minh N Van, Cao Y, Nogami M. The development of mixture, alloy, and core-shell nanocatalysts with nanomaterial supports for energy conversion in low-temperature fuel cells. Nano Energy [Internet]. 2013;2(5):636–76. Available from: http://dx.doi.org/10.1016/j.nanoen.2013.06.001

95. Li G, Tang Z. Noble metal nanoparticle@metal oxide core/yolk-shell nanostructures as catalysts: Recent progress and perspective. Nanoscale. 2014;6(8):3995–4011.

96. Ghosh Chaudhuri R, Paria S. Core/shell nanoparticles: Classes, properties, synthesis mechanisms, characterization, and applications. Chem Rev. 2012;112(4):2373–433.

97. Yu J, Wang Q, O'Hare D, Sun L. Preparation of two dimensional layered double hydroxide nanosheets and their applications. Chem Soc Rev. 2017;46(19):5950–74.

98. Park M, Lee C-I, Lee E-J, Choy J-H, Kim J-E, Choi J. Layered double hydroxides as potential solid base for beneficial remediation of endosulfan-contaminated soils. J Phys Chem Solids. 2004;65(2–3):513–6.

99. Olya N, Ghasemi E, Mahdavian M, Ramezanzadeh B. Construction of a novel corrosion protective composite film based on a core-shell LDH-Mo@ SiO2 inhibitor nanocarrier with both self-healing/barrier functions. J Taiwan Inst Chem Eng. 2020;113:406–18.

100. He J, Yang Z, Zhang L, Li Y, Pan L. Cu supported on ZnAl-LDHs precursor prepared by in-situ synthesis method on γ-Al2O3 as catalytic material with high catalytic activity for methanol steam reforming. Int J Hydrogen Energy. 2017;42(15):9930–7.

101. Erickson KL, Bostrom TE, Frost RL. A study of structural memory effects in synthetic hydrotalcites using environmental SEM. Mater Lett. 2005;59(2–3):226–9.

102. Soheili-Azad P, Yaftian MR, Dorraji MSS. Application of zinc/aluminum layered double hydroxide nanosorbent in a fixed-bed column for SPE-preconcentration followed by HPLC determination of diclofenac in biological and hospital wastewater samples. Microchem J. 2019;148:270–6.

103. Saikia J, Bordoloi P, Yadav A, Pal M, Goswamee RL. Layered double hydroxide and microwave assisted functionalized carbon based nanocomposites as controlled release vehicle for antibiotics. J Drug Deliv Sci Technol. 2019;49:243–53.

104. Feng X, Yu Z, Long R, Li X, Shao L, Zeng H, et al. Self-assembling 2D/2D (MXene/LDH) materials achieve ultra-high adsorption of heavy metals Ni2+ through terminal group modification. Sep Purif Technol. 2020;253:117525.

105. Lu P, Liu Y, Zhou T, Wang Q, Li Y. Recent advances in layered double hydroxides (LDHs) as two-dimensional membrane materials for gas and liquid separations. J Memb

Sci. 2018;567:89–103.

106. Kuthati Y, Kankala RK, Lee C-H. Layered double hydroxide nanoparticles for biomedical applications: Current status and recent prospects. Appl Clay Sci. 2015;112:100–16.

107. Su LW, Lin DJ, Uan JY. Novel dental resin composites containing LiAl-F layered double hydroxide (LDH) filler: Fluoride release/recharge, mechanical properties, color change, and cytotoxicity. Dent Mater. 2019;35(5):663–72.

108. Van den Bossche S, Vandeplassche E, Ostyn L, Coenye T, Crabbé A. Bacterial interference with lactate dehydrogenase assay leads to an underestimation of cytotoxicity. Front Cell Infect Microbiol. 2020;494.

109. Pawlak J, Trzcionka A, Mertas A, Dziedzic A, Hildebrandt T, Tanasiewicz M. The Cytotoxicity Assessment of Novel Formulation Developed to Reduce Dentin Hypersensitivity Utilizing Dehydrogenase Assay. Coatings. 2021;11(2):217.

110. LEROUX F, BESSE J-P. Layered double hydroxide/polymer nanocomposites. In: Interface Science and Technology. Elsevier; 2004. p. 459–95.

111. Zhao Y, Li F, Zhang R, Evans DG, Duan X. Preparation of layered double-hydroxide nanomaterials with a uniform crystallite size using a new method involving separate nucleation and aging steps. Chem Mater. 2002;14(10):4286–91.

112. Gardner E, Huntoon KM, Pinnavaia TJ. Direct synthesis of alkoxide-intercalated derivatives of hydrocalcite-like layered double hydroxides: precursors for the formation of colloidal layered double hydroxide suspensions and transparent thin films. Adv Mater. 2001;13(16):1263–6.

113. Géraud E, Prévot V, Ghanbaja J, Leroux F. Macroscopically ordered hydrotalcite-type materials using self-assembled colloidal crystal template. Chem Mater. 2006;18(2):238–40.

114. Patterson AL. The Scherrer formula for X-ray particle size determination. Phys Rev. 1939;56(10):978.

115. Mishra G, Dash B, Pandey S. Layered double hydroxides: A brief review from fundamentals to application as evolving biomaterials. Appl Clay Sci. 2018;153:172–86.

116. Taylor RM. The rapid formation of crystalline double hydroxy salts and other compounds by controlled hydrolysis. Clay Miner. 1984;19(4):591–603.

117. Indira L, Dixit M, Kamath PV. Electrosynthesis of layered double hydroxides of nickel with trivalent cations. J Power Sources. 1994;52(1):93–7.

118. Lopez T, Bosch P, Ramos E, Gomez R, Novaro O, Acosta D, et al. Synthesis and characterization of sol− gel hydrotalcites. Structure and texture. Langmuir. 1996;12(1):189–92.

119. Wang JA, Bokhimi X, Morales A, Novaro O, Lopez T, Gomez R. Aluminum local environment and defects in the crystalline structure of Sol− Gel alumina catalyst. J Phys Chem B. 1999;103(2):299–303.

120. Kooli F, Depege C, Ennaqadi A, De Roy A, Besse JP. Rehydration of Zn-Al layered double hydroxides. Clays Clay Miner. 1997;45:92–8.

121. Crepaldi EL, Pavan PC, Valim JB. A new method of intercalation by anion exchange in layered double hydroxides. Chem Commun. 1999;(2):155–6.

122. Abdolmohammad-Zadeh H, Rezvani Z, Sadeghi GH, Zorufi E. Layered double hydroxides: A novel nano-sorbent for solid-phase extraction. Anal Chim Acta [Internet]. 2011;685(2):212–9. Available from: https://www.sciencedirect.com/science/article/pii/S0003267010014509

123. Asif M, Aziz A, Wang H, Wang Z, Wang W, Ajmal M, et al. Superlattice stacking by hybridizing layered double hydroxide nanosheets with layers of reduced graphene oxide for electrochemical simultaneous determination of dopamine, uric acid and ascorbic acid. Microchim Acta. 2019;186:1–11.

124. Jabeen M, Ishaq M, Song W, Xu L, Deng Q. Synthesis of Ni/Co/Al-layered triple hydroxide@ brominated graphene hybrid on nickel foam as electrode material for high-performance supercapacitors. RSC Adv. 2017;7(74):46553–65.

125. Song L, Shi W, Lu C. Confinement Effect in Layered Double Hydroxide Nanoreactor: Improved Optical Sensing Selectivity. Anal Chem [Internet]. 2016 Aug 16;88(16):8188–93. Available from: https://doi.org/10.1021/acs.analchem.6b02000

126. Cao Y, Zheng D, Zhang F, Pan J, Lin C. Layered double hydroxide (LDH) for multi-functionalized corrosion protection of metals: A review. J Mater Sci Technol. 2022;102:232–63.

127. Bradley DC, Mehrotra RC, Gaur DP. Metal alkoxides [Internet]. United Kingdom: Academic Press; 1978. Available from: http://inis.iaea.org/search/search.aspx?orig_q=RN:16016987

128. Rogojan R, Andronescu E, Ghitulica C, Birsan M, Voicu G, Stoleriu S, et al. Analysis of the structure and morphology of hydroxyapatite nanopowder obtained by sol-gel and pirosol methods. In: Advanced Materials Research. Trans Tech Publ; 2012. p. 63–7.

129. Bahuguna G, Mishra NK. Thin film coating. Res J Chem. 2016;6(7):65–72.

130. Gupta SM, Tripathi M. A review on the synthesis of TiO 2 nanoparticles by solution route. Cent Eur J Chem. 2012;10:279–94.

131. Yoldas BE. Monolithic glass formation by chemical polymerization. J Mater Sci. 1979;14:1843–9.

132. Scherer GW. Aging and drying of gels. J Non Cryst Solids. 1988;100(1–3):77–92.

133. Isley SL, Penn RL. Titanium dioxide nanoparticles: Effect of sol− gel pH on phase composition, particle size, and particle growth mechanism. J Phys Chem C. 2008;112(12):4469–74.

134. de Coelho Escobar C, dos Santos JHZ. Effect of the sol–gel route on the textural characteristics of silica imprinted with Rhodamine B. J Sep Sci. 2014;37(7):868–75.

135. Kajihara K. Recent advances in sol-gel synthesis of monolithic silica and silica-based glasses. J Asian Ceram Soc 1 (2): 121–133. 2013.

136. Parashar M, Shukla VK, Singh R. Metal oxides nanoparticles via sol–gel method: a review on synthesis, characterization and applications. J Mater Sci Mater Electron. 2020;31:3729–49.

137. Hench LL. JK West The sol-gel process Chem. Rev. 1990;90:33–72.

138. Niederberger M, Pinna N. Metal oxide nanoparticles in organic solvents: synthesis, formation, assembly and application. Springer Science & Business Media; 2009.

139. Collinson MM, Wang H, Makote R, Khramov A. The effects of drying time and relative humidity on the stability of sol–gel derived silicate films in solution. J Electroanal Chem. 2002;519(1–2):65–71.

140. Kumar A, Yadav N, Bhatt M, Mishra NK, Chaudhary P, Singh R. Sol-gel derived nanomaterials and it's applications: a review. Res J Chem Sci _____ ISSN. 2015;2231:606X.

141. Mackenzie JD. Applications of the sol-gel process. J Non Cryst Solids. 1988;100(1–

3):162–8.

142. Deng Z, Wang J, Wei J, Shen J, Zhou B, Chen L. Physical properties of silica aerogels prepared with polyethoxydisiloxanes. J Sol-Gel Sci Technol. 2000;19:677–80.

143. Rao AV, Bhagat SD, Hirashima H, Pajonk GM. Synthesis of flexible silica aerogels using methyltrimethoxysilane (MTMS) precursor. J Colloid Interface Sci. 2006 Aug;300(1):279–85.

144. El Rassy H, Buisson P, Bouali B, Perrard A, Pierre AC. Surface characterization of silica aerogels with different proportions of hydrophobic groups, dried by the CO2 supercritical method. Langmuir. 2003;19(2):358–63.

145. Harreld JH, Ebina T, Tsubo N, Stucky G. Manipulation of pore size distributions in silica and ormosil gels dried under ambient pressure conditions. J Non Cryst Solids. 2002;298(2–3):241–51.

146. Kistler SS. Coherent expanded aerogels. Rubber Chem Technol. 1932;5(4):600–3.

147. Bala N, Khosla C. Preparation and deposition of hydroxyapatite on biomaterials by sol-gel technique-a review. 2014;

148. Brinker CJ, Scherer GW. Sol-gel science: the physics and chemistry of sol-gel processing. Academic press; 2013.

149. Malato S, Fernández-Ibáñez P, Maldonado MI, Blanco J, Gernjak W. Decontamination and disinfection of water by solar photocatalysis: recent overview and trends. Catal today. 2009;147(1):1–59.

150. Yang L, Dai Q, Liu L, Shao D, Luo K, Jamil S, et al. Rapid sintering method for highly conductive Li7La3Zr2O12 ceramic electrolyte. Ceram Int. 2020;46(8):10917–24.

151. Li Z, Shi Y, Zhu A, Zhao Y, Wang H, Binks BP, et al. Light-responsive, reversible emulsification and demulsification of oil-in-water pickering emulsions for catalysis. Angew Chemie. 2021;133(8):3974–9.

152. Kang J, Um W. Use of Layered Double Hydroxide (LDH) Sorbents to Remove Radioactive Iodine Species–17178. In WM Symposia, Inc., PO Box 27646, 85285-7646 Tempe, AZ (United States); 2017.

153. Jiang S, Liu Y, Xie W, Shao M. Electrosynthesis of hierarchical NiLa-layered double hydroxide electrode for efficient oxygen evolution reaction. J Energy Chem [Internet]. 2019;33:125–9. Available from: https://www.sciencedirect.com/science/article/pii/S2095495618307034

154. Liu L, Cheng M, Yang Z. Improved performance of flower-like ZnAl LDH growing on carbon nanotubes used in zinc–nickel secondary battery. Electrochim Acta. 2018;277:67–76.

155. Yasaei M, Khakbiz M, Zamanian A, Ghasemi E. Synthesis and characterization of Zn/Al-LDH@ SiO2 nanohybrid: Intercalation and release behavior of vitamin C. Mater Sci Eng C. 2019;103:109816.

156. Xie F, Ma L, Gan M, He H, Hu L, Jiang M, et al. One-pot construction of the carbon spheres embellished by layered double hydroxide with abundant hydroxyl groups for Pt-based catalyst support in methanol electrooxidation. J Power Sources. 2019;420:73–81.

157. Li F, Sun Z, Jiang H, Ma Z, Wang Q, Qu F. Ion-exchange synthesis of ternary FeCoNi-layered double hydroxide nanocage toward enhanced oxygen evolution reaction and supercapacitor. Energy & Fuels. 2020;34(9):11628–36.

158. Hu H, Wageh S, Al-Ghamdi AA, Yang S, Tian Z, Cheng B, et al. NiFe-LDH nanosheet/carbon fiber nanocomposite with enhanced anionic dye adsorption performance.

Appl Surf Sci. 2020;511:145570.

159. Guo L, Zhang Y, Zheng J, Shang L, Shi Y, Wu Q, et al. Synthesis and characterization of ZnNiCr-layered double hydroxides with high adsorption activities for Cr (VI). Adv Compos Hybrid Mater. 2021;4(3):819–29.

160. Zhou Y-N, Wang F-L, Dou S-Y, Shi Z-N, Dong B, Yu W-L, et al. Motivating high-valence Nb doping by fast molten salt method for NiFe hydroxides toward efficient oxygen evolution reaction. Chem Eng J. 2022;427:131643.

161. Kang G-H, Park I-K. Reconstruction and intercalating anion exchange of ZnAl-layered double hydroxide. Ceram Int. 2022;48(3):3030–6.

162. Beigi F, Mahjoub AR, Khavar AHC. Design and synthesis of Bi-doped NiAl-LDH/g-C3N4 heterostructure; a novel 2D/2D system for simultaneous enhanced photocatalytic degradation and fluorescence sensing of ciprofloxacin. Appl Surf Sci. 2023;637:157972.

163. Carlino S, Hudson MJ, Husain SW, Knowles JA. The reaction of molten phenylphosphonic acid with a layered double hydroxide and its calcined oxide. Solid State Ionics. 1996;84(1–2):117–29.

164. Carlino S, Hudson MJ. Reaction of molten sebacic acid with a layered (Mg/Al) double hydroxide. J Mater Chem. 1994;4(1):99–104.

165. Jabłońska M, Chmielarz L, Węgrzyn A, Guzik K, Piwowarska Z, Witkowski S, et al. Thermal transformations of Cu–Mg (Zn)–Al(Fe) hydrotalcite-like materials into metal oxide systems and their catalytic activity in selective oxidation of ammonia to dinitrogen. J Therm Anal Calorim [Internet]. 2013;114(2):731–47. Available from: https://doi.org/10.1007/s10973-012-2935-9

166. Valeikiene L, Grigoraviciute-Puroniene I, Katelnikovas A, Zarkov A, Kareiva A. Investigation of Structural and Luminescent Properties of Sol-Gel-Derived Cr-Substituted Mg3Al1− xCrx Layered Double Hydroxides. Molecules. 2021;26(7):1848.

167. Haraketi M, Hosni K, Srasra E. Intercalation behavior of salicylic acid into calcined Cu-Al-layered double hydroxides for a controlled release formulation. Surf Eng Appl Electrochem. 2017;53:360–70.

168. Wang H, Chen Y, Xie W, Han X, Feng Q, Jiang R, et al. Construction of Highly Active Pt/Ni-Fe Layered Double Hydroxide Electrocatalyst towards Methanol Oxidation in Alkaline Medium. Int J Electrochem Sci [Internet]. 2019;14(8):7961–72. Available from: https://www.sciencedirect.com/science/article/pii/S1452398123013925

169. Gamil S, El Rouby WMA, Antuch M, Zedan IT. Nanohybrid layered double hydroxide materials as efficient catalysts for methanol electrooxidation. RSC Adv [Internet]. 2019;9(24):13503–14. Available from: http://dx.doi.org/10.1039/C9RA01270B

170. Karthik K, Dhanuskodi S, Gobinath C, Prabukumar S, Sivaramakrishnan S. Multifunctional properties of microwave assisted CdO–NiO–ZnO mixed metal oxide nanocomposite: enhanced photocatalytic and antibacterial activities. J Mater Sci Mater Electron. 2018;29:5459–71.

171. Ma K, Cheng JP, Liu F, Zhang X. Co-Fe layered double hydroxides nanosheets vertically grown on carbon fiber cloth for electrochemical capacitors. J Alloys Compd. 2016;679:277–84.

172. Badreddine M, Khaldi M, Legrouri A, Barroug A, Chaouch M, De Roy A, et al. Chloride-hydrogenophosphate ion exchange into the zinc–aluminium–chloride layered double hydroxide. Mater Chem Phys. 1998;52(3):235–9.

173. Dimitriev Y, Ivanova Y, Iordanova R. History of sol-gel science and technology. J Univ Chem Technol Metall. 2008;43(2):181–92.